

**Supplementary information for**

# **Mono- and dinuclear tetraphosphabutadiene ferrate anions**

*Uttam Chakraborty, Julia Leitl, Bernd Mühldorf, Michael Bodensteiner, Stefan Pelties and  
Robert Wolf\**

University of Regensburg, Institute of Inorganic Chemistry, D-93040 Regensburg;

E-mail: [robert.wolf@ur.de](mailto:robert.wolf@ur.de); <http://www.uni-regensburg.de/chemistry-pharmacy/inorganic-chemistry-wolf/index.html>

## **Table of Contents**

1	Experimental Section.....	2
1.1	General considerations .....	2
1.2	Synthesis of [K(18-crown-6){Cp <sup>Ar</sup> Fe(P <sub>4</sub> )}] (2) .....	2
1.3	Synthesis of [Na <sub>2</sub> (THF) <sub>5</sub> {(Cp <sup>Ar</sup> Fe) <sub>2</sub> (P <sub>4</sub> )}] (3).....	5
1.4	Synthesis of [Na(THF) <sub>3</sub> {(Cp <sup>Ar</sup> Fe) <sub>2</sub> (H)(P <sub>4</sub> )}] (4) .....	9
1.5	Reaction of 3 with Me <sub>3</sub> SiCl .....	14
2	Crystallographic data for complexes 2, 3 and 4 .....	15
2.1	Crystallographic Data of 2 .....	16
2.2	Crystallographic Data of 3 .....	16
2.3	Crystallographic Data for 4.....	16
3	DFT calculations.....	18
3.2	Calculated frontier molecular orbitals of 2' .....	19
3.3	Optimization of isomers of Na[CpFe <sub>2</sub> P <sub>4</sub> H] (4A) .....	20
3.4	Calculated energy profile for the fluxional behaviour of 4A.....	20
3.6	TD-DFT calculations for complex 2' .....	21
4	Cartesian coordinates of the optimized structures.....	22
4.1	Cartesian coordinates of 2'.....	22
4.2	Cartesian coordinates of 4' (optimized at the B3LYP/def2-TZVP level of theory) .....	23
4.3	Cartesian Coordinates of 4A.....	25
4.4	Cartesian Coordinates of 4B .....	26

## 1 Experimental Section

### 1.1 General considerations

Strictly anaerobic conditions are required for the synthesis of compound **1 – 4**. All experiments were performed under an atmosphere of dry argon, by using standard Schlenk and glovebox techniques. Solvents were purified, dried, and degassed with an MBraun SPS800 solvent purification system. NMR spectra were recorded on Avance 400 spectrometers at 300 K and internally referenced to residual solvent resonances. The  $^1\text{H}$  and  $^{13}\text{C}\{^1\text{H}\}$  NMR signals of **2**, **3** and **4** were assigned by a combination of H–H COSY, HSQC, HMBC experiments. Melting points were measured on samples in sealed capillaries on a Stuart SMP10 melting point apparatus. UV–vis spectra were recorded on a Varian Cary 50 spectrometer. Elemental analyses were determined by the analytical department of Regensburg University.  $[\text{Cp}^{\text{Ar}}\text{Fe}(\mu\text{-Br})]_2$  (**1**) was synthesized according to the literature procedures.<sup>1</sup> Sublimed [18]crown-6 was purchased from *Sigma-Aldrich* and used as received.

### 1.2 Synthesis of $[\text{K}(18\text{-crown-6})\{\text{Cp}^{\text{Ar}}\text{Fe}(\text{P}_4)\}]$ (**2**)

A deep yellow solution of **1** (1.03g, 0.715 mmol) and [18]crown-6 (732 mg, 2.77 mmol) in 15 mL of THF was added to the green potassium naphthalenide solution [prepared from 111 mg (2.84 mmol) of K and 364 mg (2.84 mmol) naphthalene in 10 mL of THF during 16 hours] at – 80 °C over 30 min. A deep orange mixture was observed, which was treated with a solution of white P<sub>4</sub> (185 mg, 1.49 mmol) in 15 mL THF over 15 min. The obtained orange-brown suspension was allowed to reach room temperature in two hours, affording a greenish brown suspension. It was immediately filtered through a P<sub>4</sub> frit. The greenish filtrate was layered with 25 mL of *n*-hexane and stored at – 30 °C for two days, affording a greenish crystalline solid, which was isolated and washed with 2 × 10 mL diethyl ether. In order to remove remaining Cp<sup>Ar</sup>K, the residue taken up in 10 mL of benzene and filtered. The emerald green filtrate was evaporated completely to afford a light green solid. Yield: 65 mg (0.061 mmol, 4 %); m.p. >239 °C (decomposition to a black solid). UV–vis (THF):  $\lambda_{\text{max}}$  /nm ( $\varepsilon_{\text{max}}$  / L·mol<sup>−1</sup>·cm<sup>−1</sup>) = 405 (sh, 2800), 653 (553).  $^1\text{H}$  NMR (400.13 MHZ, THF-d<sub>8</sub>, 300 K): 1.12 (t,  $^3J$  = 8.0 Hz, 15H, 5 × CH<sub>3</sub>, Cp<sup>Ar</sup>), 2.46 (q,  $^3J$  = 8.0 Hz, 10H, 5 × CH<sub>2</sub>, Cp<sup>Ar</sup>), 3.66 (s, 24H, [18]crown-6), 6.63 (d,

$^3J = 8.0$  Hz, 10H,  $5 \times m\text{-}CH$ , Cp<sup>Ar</sup>), 7.24 (d,  $^3J = 8.0$  Hz, 10H,  $5 \times o\text{-}CH$ , Cp<sup>Ar</sup>);  $^{31}\text{P}\{\text{H}\}$  NMR (161.98 MHZ, THF-d<sub>8</sub>, 300 K): 114.1;  $^{13}\text{C}\{\text{H}\}$  NMR (100.61 MHZ, C<sub>6</sub>D<sub>6</sub>, 300 K): 15.5 (s, CH<sub>3</sub>, Cp<sup>Ar</sup>), 29.1 (s, CH<sub>2</sub>, Cp<sup>Ar</sup>), 71.2 (s, CH<sub>2</sub>, [18]crown-6), 92.9 (s, C<sub>ring</sub> carbon atoms of Cp<sup>Ar</sup>), 125.8 (s, m-CH, Cp<sup>Ar</sup>), 134.6 (s, C<sub>ipso</sub>, Cp<sup>Ar</sup>), 137.8 (s, o-CH, Cp<sup>Ar</sup>), 140.1 (s, p-C, Cp<sup>Ar</sup>); elemental analysis calcd. for (C<sub>57</sub>H<sub>69</sub>FeP<sub>4</sub>KO<sub>6</sub>)·0.2(C<sub>6</sub>H<sub>6</sub>) (Mw = 1100.55 g/mol): C 64.84, H 6.45; found: C 65.07, H 6.42.

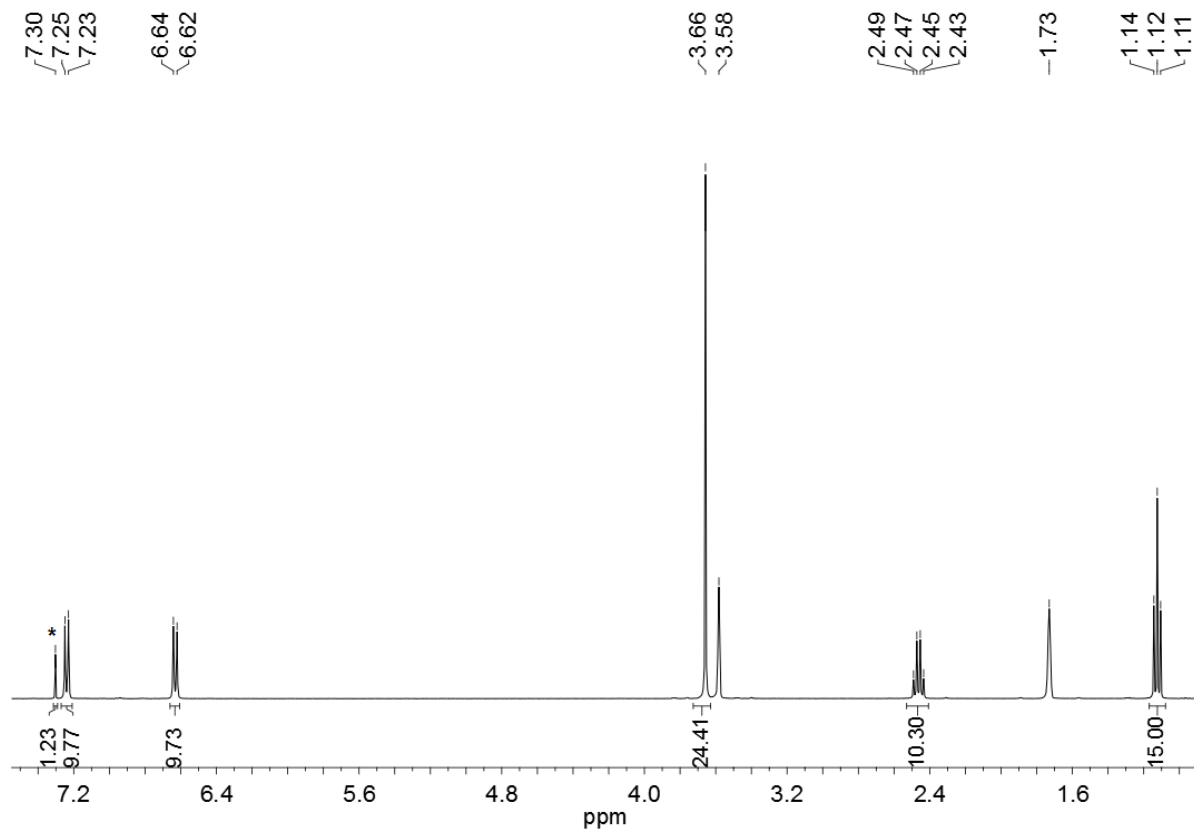


**Figure S1.**  $^1\text{H}$  NMR spectrum of complex **2** (400.13 MHz, THF-d<sub>8</sub>, 300 K); \* denotes the signal corresponding to benzene.

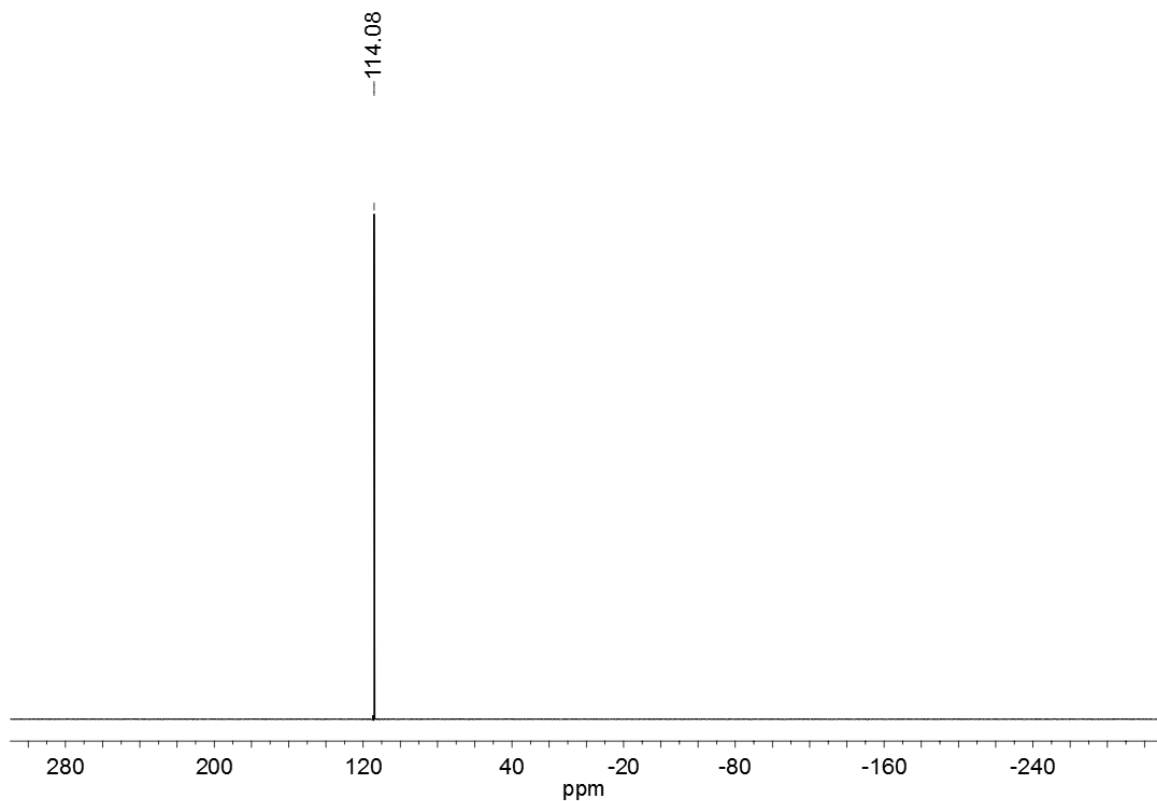


**Figure S2.**  $^{31}\text{P}\{\text{H}\}$  NMR spectrum of complex **2** (161.98 MHz, THF-d<sub>8</sub>, 300 K).

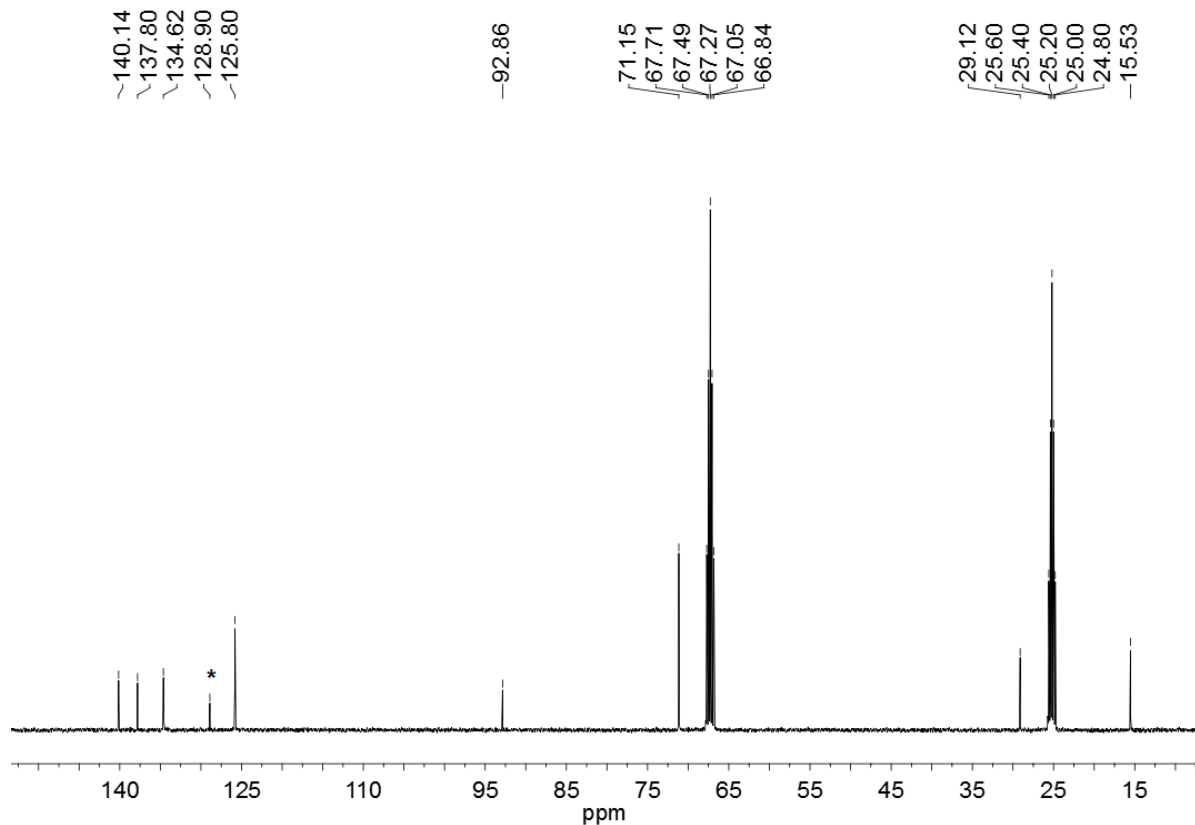


**Figure S3.**  $^{13}\text{C}\{\text{H}\}$  NMR spectrum of complex **2** (100.61 MHz, THF-d<sub>8</sub>, 300 K); \* denotes the signal corresponding to benzene.

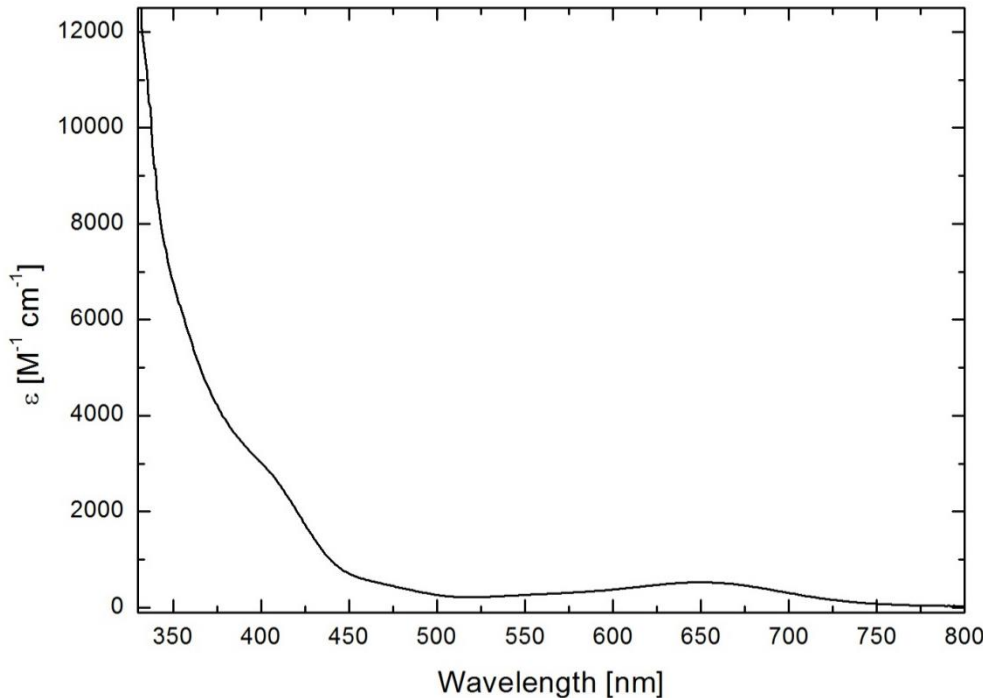


**Figure S4.** UV-vis spectrum of **2** in THF.

### 1.3 Synthesis of $[\text{Na}_2(\text{THF})_5\{(\text{Cp}^{\text{Ar}}\text{Fe})_2(\text{P}_4)\}]$ (**3**)

A mixture of **1** (500 mg, 0.345 mmol) and white P<sub>4</sub> (86 mg, 0.69 mmol) was dissolved in 40 mL of THF. The yellowish solution was treated with Na/Hg (5 mL of 0.5 wt%, 14.8 mmol) at room temperature under vigorous stirring. The color of the mixture turned to red brown, and the reaction mixture was stirred for four hours. The obtained red suspension was decanted from Hg and filtered through a P4 frit. The red filtrate was concentrated to 5 mL and layered with 8 mL of diethyl ether. Complex **3** was obtained as a dark brown-red solid after crystallization at -35 °C for two days. Yield: 420 mg (67%, 0.231 mmol). The compound is stable as a crystalline solid, but slowly decomposes in THF solution over several days. The formation of several decomposition products is observed by <sup>31</sup>P NMR spectroscopy, including the putative radical anion  $\text{Na}[(\text{Cp}^{\text{Ar}}\text{Fe})_2(\mu\text{-P}_4)]$  and the protonated product **4**. UV-vis (THF):  $\lambda_{\text{max}}$  /nm ( $\epsilon_{\text{max}}$  / L·mol<sup>-1</sup>·cm<sup>-1</sup>) = 325 (13290), 356 (11460), 452 (4317); M.p. > 300 °C (no decomposition until 300 °C). <sup>1</sup>H NMR (400.13 MHZ, C<sub>6</sub>D<sub>6</sub>, 300 K): 1.02 (t, <sup>3</sup>J = 8.0 Hz, 30H, 5 × CH<sub>3</sub>, Cp<sup>Ar</sup>), 1.45 (s br, THF), 2.35 (q, <sup>3</sup>J = 8.0 Hz, 20H, 5 × CH<sub>2</sub>, Cp<sup>Ar</sup>), 3.51 (s br, THF), 6.80 (d, <sup>3</sup>J = 8.0 Hz, 20H, 5 × m-CH, Cp<sup>Ar</sup>), 7.84 (d, <sup>3</sup>J = 8.0 Hz, 20H, 5 × o-CH, Cp<sup>Ar</sup>); <sup>31</sup>P{<sup>1</sup>H} NMR (161.98 MHZ, C<sub>6</sub>D<sub>6</sub>, 300 K): -135.4; <sup>31</sup>P{<sup>1</sup>H} NMR (161.98 MHZ, THF-d<sub>8</sub>, 300 K): -130.0; <sup>13</sup>C{<sup>1</sup>H}NMR (100.61 MHZ, C<sub>6</sub>D<sub>6</sub>, 300 K): 15.1 (s, CH<sub>3</sub>, Cp<sup>Ar</sup>), 25.7 (s, THF), 28.7

(s,  $\text{CH}_2$ ,  $\text{Cp}^{\text{Ar}}$ ), 67.9 (s, THF), 88.7 (s,  $\text{Cp}_{\text{ring}}$  carbon atoms of  $\text{Cp}^{\text{Ar}}$ ), 125.85 (s, *m*-CH,  $\text{Cp}^{\text{Ar}}$ ), 133.8 (s,  $\text{C}_{\text{ipso}}$ ,  $\text{Cp}^{\text{Ar}}$ ), 137.7 (s, *o*-CH,  $\text{Cp}^{\text{Ar}}$ ), 139.25 (s, *p*-C,  $\text{Cp}^{\text{Ar}}$ ); elemental analysis calcd. for  $\text{C}_{110}\text{H}_{130}\text{Fe}_2\text{Na}_2\text{O}_5\text{P}_4$  ( $\text{Mw} = 1813.81$  g/mol): C 72.84, H 7.22; found: C 73.40, H 7.47.

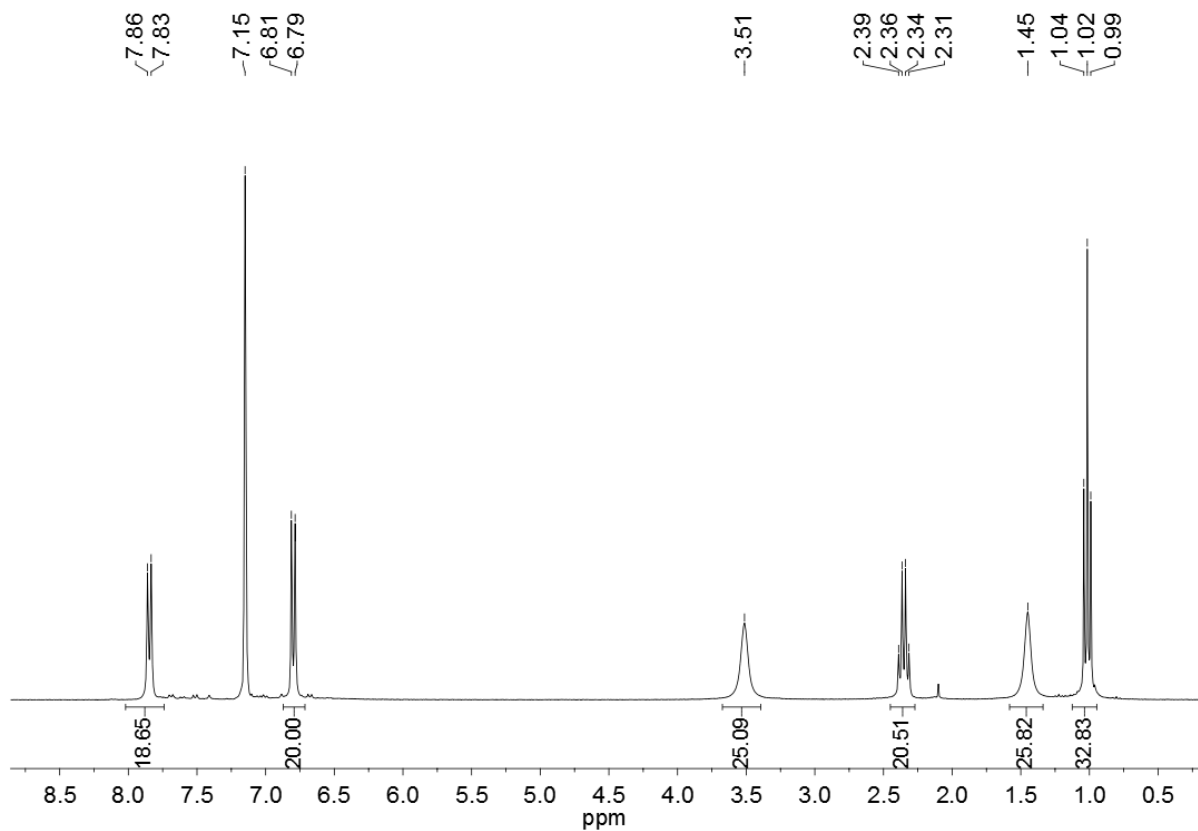


**Figure S5.**  $^1\text{H}$  NMR spectrum of complex **3** (400.13 MHz,  $\text{C}_6\text{D}_6$ , 300 K).

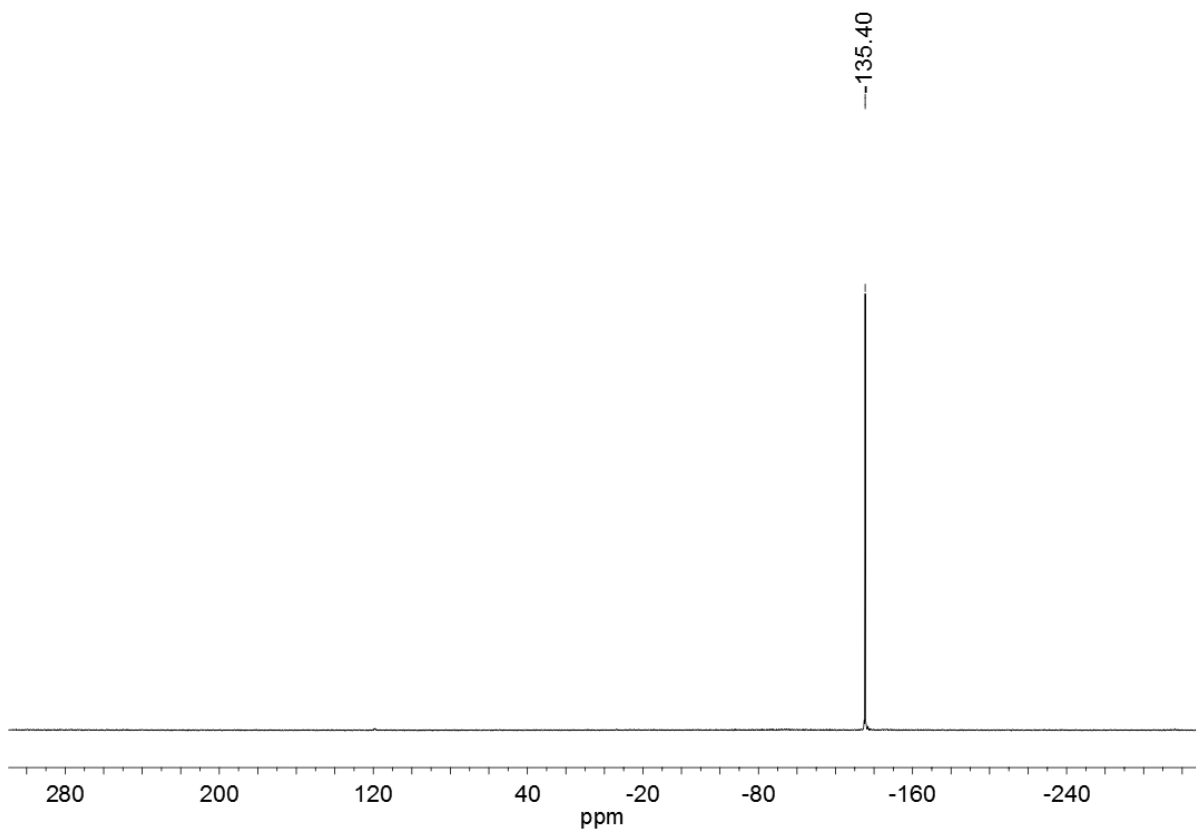


**Figure S6.**  $^{31}\text{P}\{\text{H}\}$  NMR spectrum of complex **3** (161.98 MHz,  $\text{C}_6\text{D}_6$ , 300 K).

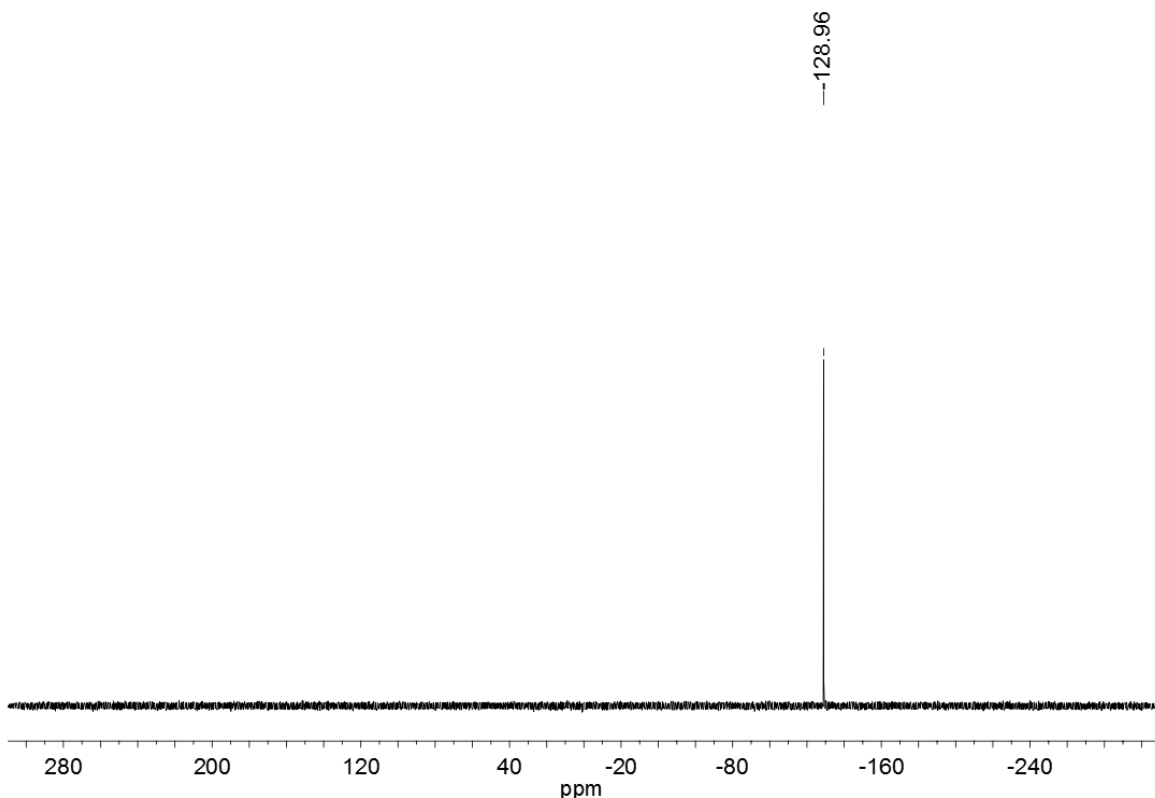


**Figure S7.**  $^{31}\text{P}\{\text{H}\}$  NMR spectrum of complex **3** (161.98 MHz,  $\text{THF-d}_8$ , 300 K).

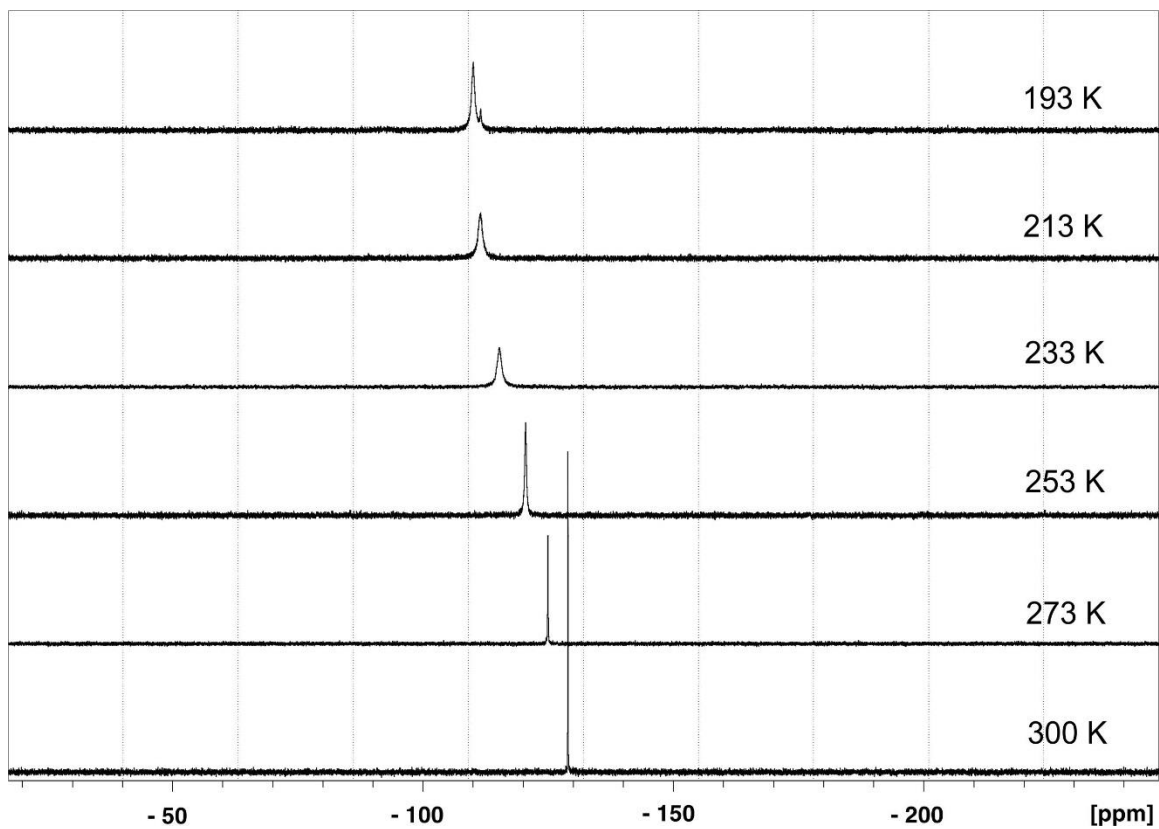


**Figure S8.** Variable temperature  $^{31}\text{P}\{\text{H}\}$  NMR spectrum of **3** (161.98 MHz, THF-d<sub>8</sub>).

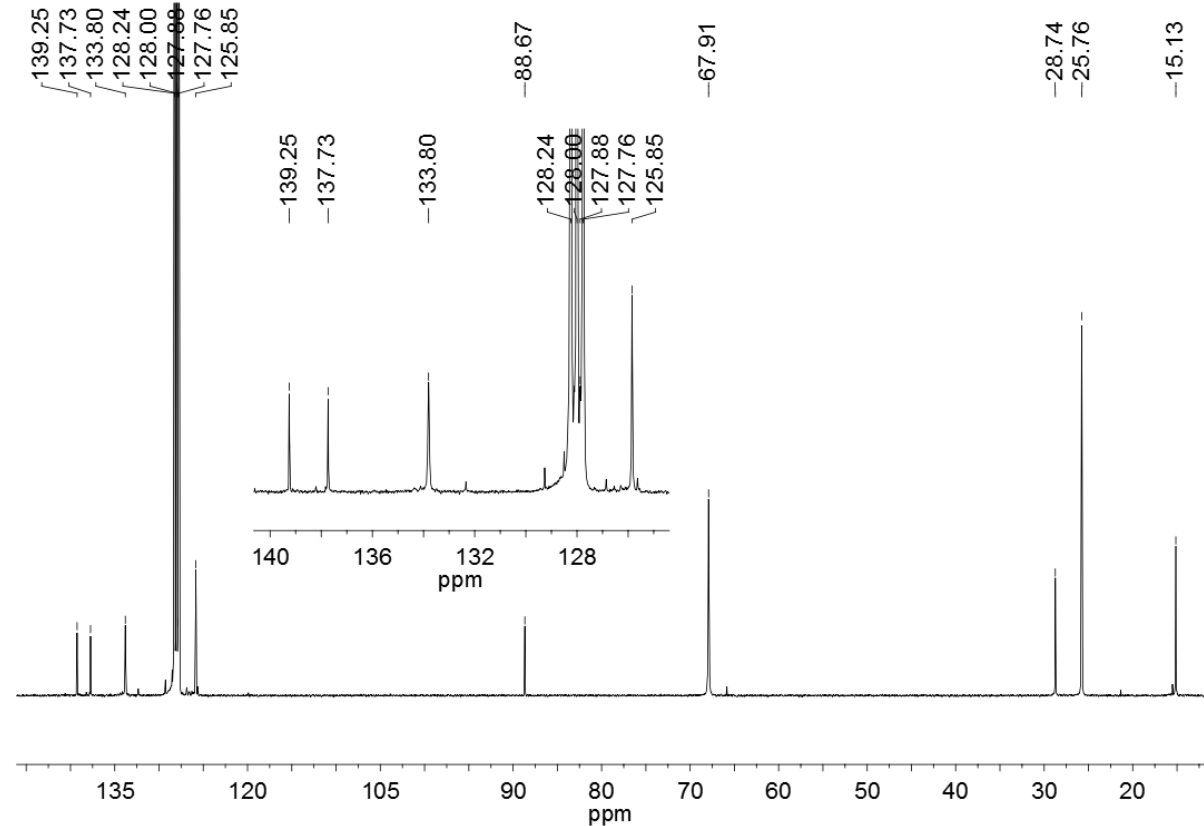


**Figure S9.**  $^{13}\text{C}\{\text{H}\}$  NMR spectrum of complex **3** (100.61 MHz, C<sub>6</sub>D<sub>6</sub>, 300 K).

#### 1.4 Synthesis of $[\text{Na}(\text{THF})_3\{(\text{Cp}^{\text{Ar}}\text{Fe})_2(\text{H})(\text{P}_4)\}]$ (4).

A mixture of **3** (188 mg, 0.10 mmol) and Et<sub>3</sub>N·HCl (15.7 mg, 0.11 mmol, 1.1 equiv.) was treated with 9 mL of THF and stirred for three hours. The brown mixture turned to green-brown. Afterwards, the reaction mixture was filtered. The filtrate was evaporated completely to dryness and extracted with 5 x 2 mL of toluene. The brown toluene solution was evaporated completely to dryness and the brown residue was dissolved in 2 mL of THF. Complex **4** was isolated as a red-brown solid after layering a THF solution with 8 mL of *n*-hexane and storage at room temperature for two days. Yield: 75 mg (0.1 mmol, 44%). The isolated compound may still be the putative paramagnetic complex Na[(Cp<sup>Ar</sup>Fe)<sub>2</sub>(μ-P<sub>4</sub>)] as a by-product. This paramagnetic complex can be identified by broad <sup>1</sup>H NMR signals at 6.57 and 2.57 ppm. The impurity can be removed by recrystallization from THF/diethyl ether.

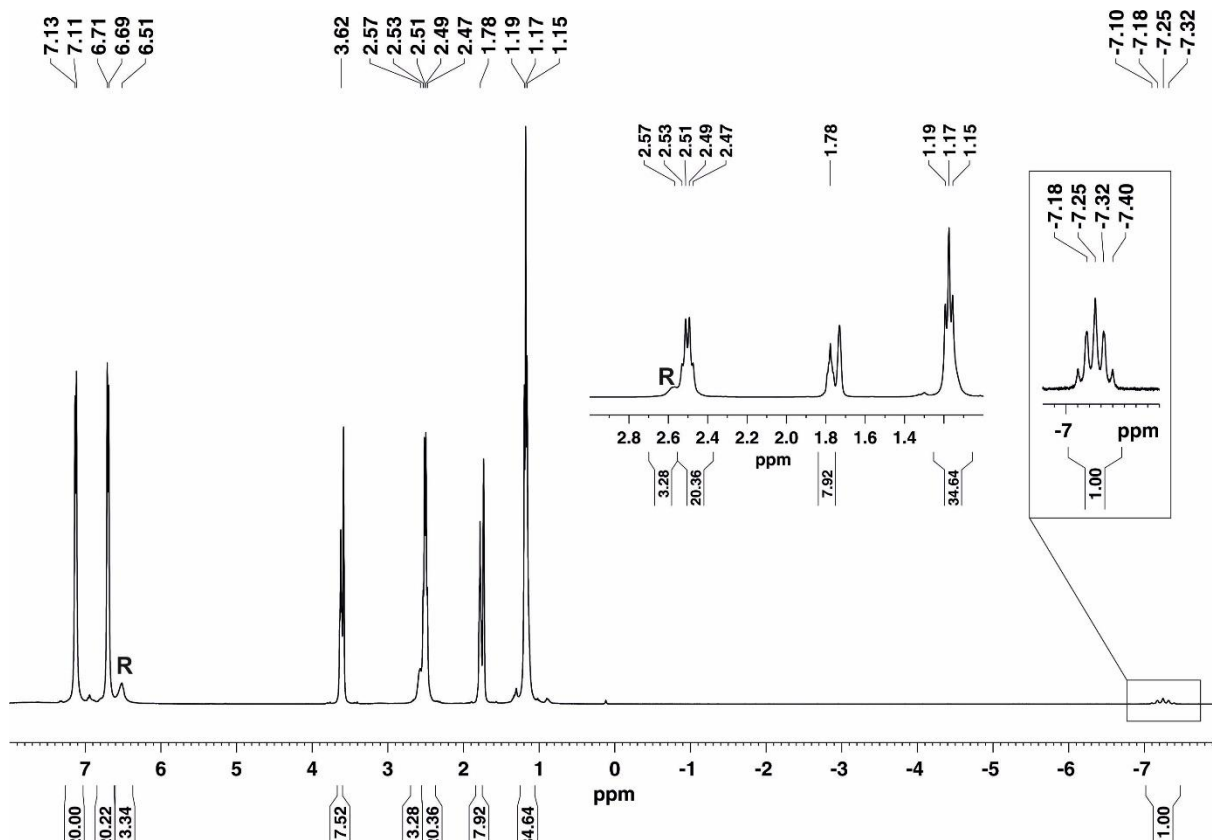


**Figure S10.**  $^1\text{H}$  NMR spectrum of complex **4** (400.13 MHz, THF- $d_8$ , 300 K); **R** denotes the radical anion  $\text{Na}[(\text{Cp}^{\text{Ar}}\text{Fe})_2(\mu-\text{P}_4)]$ .

UV-vis (THF):  $\lambda_{\text{max}}$  /nm ( $\epsilon_{\text{max}}$  / L·mol<sup>-1</sup>·cm<sup>-1</sup>) = 520 (3968); elemental analysis calcd. for C<sub>102</sub>H<sub>115</sub>Fe<sub>2</sub>NaO<sub>3</sub>P<sub>4</sub> (Mw = 16.47.61 g/mol): C 74.36, H 7.04; found: C 73.01, H 6.44. <sup>1</sup>H NMR (400.13 MHZ, THF-d<sub>8</sub>, 300 K): -7.21 (m,  $J_{\text{P},\text{H}} = 28$  and 32 Hz, Fe–H), 1.17 (t, <sup>3</sup>J = 7.5

Hz, 30H,  $5 \times CH_3$ , Cp<sup>Ar</sup>), 1.78 (m, THF), 2.50 (q,  $^3J = 7.3$  Hz, 20H,  $5 \times CH_2$ , Cp<sup>Ar</sup>), 3.62 (m, THF), 6.70 (d,  $^3J = 7.5$  Hz, 20H,  $5 \times m\text{-}CH$ , Cp<sup>Ar</sup>), 7.12 (d,  $^3J = 7.5$  Hz, 20H,  $5 \times o\text{-}CH$ , Cp<sup>Ar</sup>);  $^{1}H\{^{31}P\}$  NMR (400.13 MHZ, THF-d<sub>8</sub>, 300 K): -7.25 (s, Fe-H);  $^{31}P\{^{1}H\}$  NMR (161.98 MHZ, THF-d<sub>8</sub>, 300 K): 7.04 (t,  $J_{P,P} = <52$  Hz), 21.84 (t,  $J_{P,P} = 52$  Hz);  $^{31}P$  NMR (161.98 MHZ, THF-d<sub>8</sub>, 300 K): 7.20 (dt,  $J_{P,P} = 52$  Hz,  $J_{P,H} = 28$  Hz), 21.85 (dt,  $J_{P,P} = 52$  Hz,  $J_{P,H} = 32$  Hz);  $^{13}C\{^{1}H\}$  NMR (100.61 MHZ, THF-d<sub>8</sub>, 300 K): 15.4 (s,  $CH_3$ , Cp<sup>Ar</sup>), 26.3 (s, THF), 29.2 (s,  $CH_2$ , Cp<sup>Ar</sup>), 68.1 (s, THF), 87.6 (s, Cp<sub>ring</sub> carbon atoms of Cp<sup>Ar</sup>), 125.7 (s, *m*-CH, Cp<sup>Ar</sup>), 134.4 (s, *C*<sub>ipso</sub>, Cp<sup>Ar</sup>), 135.7 (s, *o*-CH, Cp<sup>Ar</sup>), 139.9 (s, *p*-C, Cp<sup>Ar</sup>).

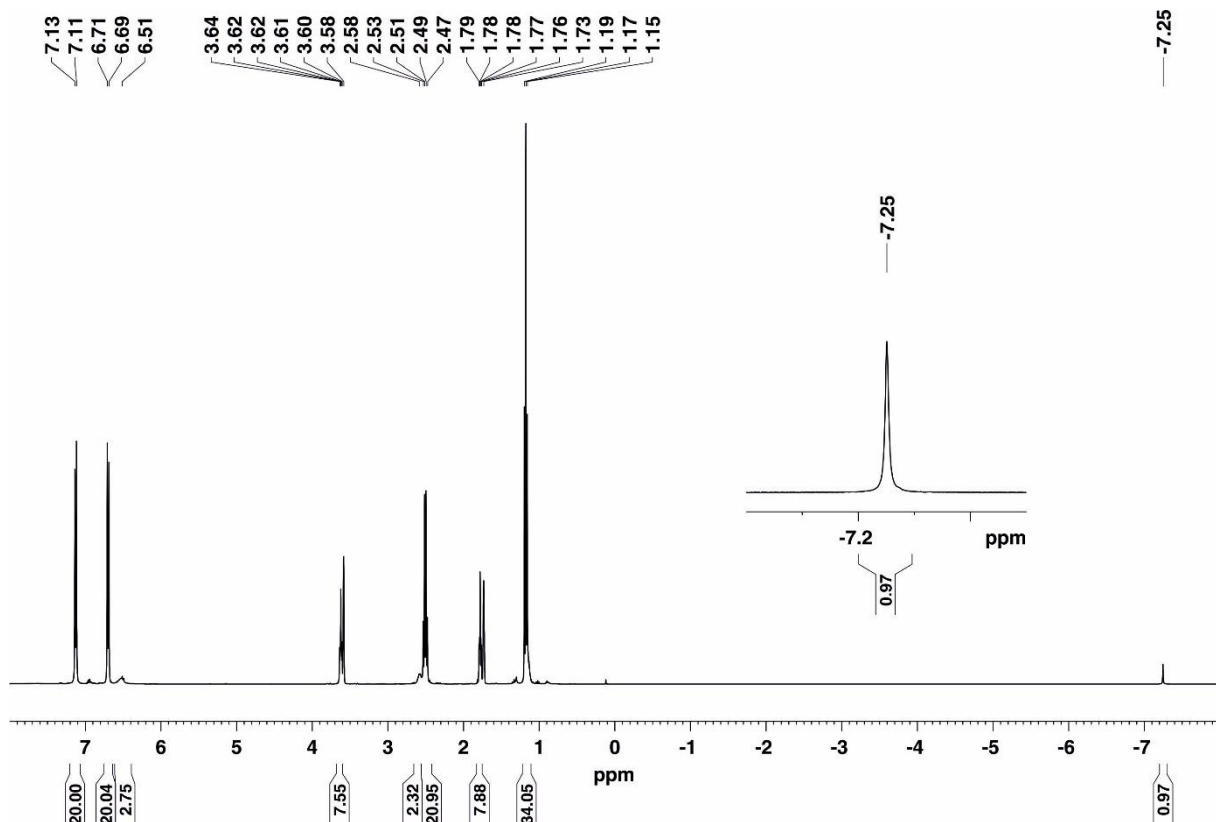


**Figure S11.**  $^{1}H\{^{31}P\}$  NMR spectrum of complex 4 (400.13 MHz, THF-d<sub>8</sub>, 300 K).

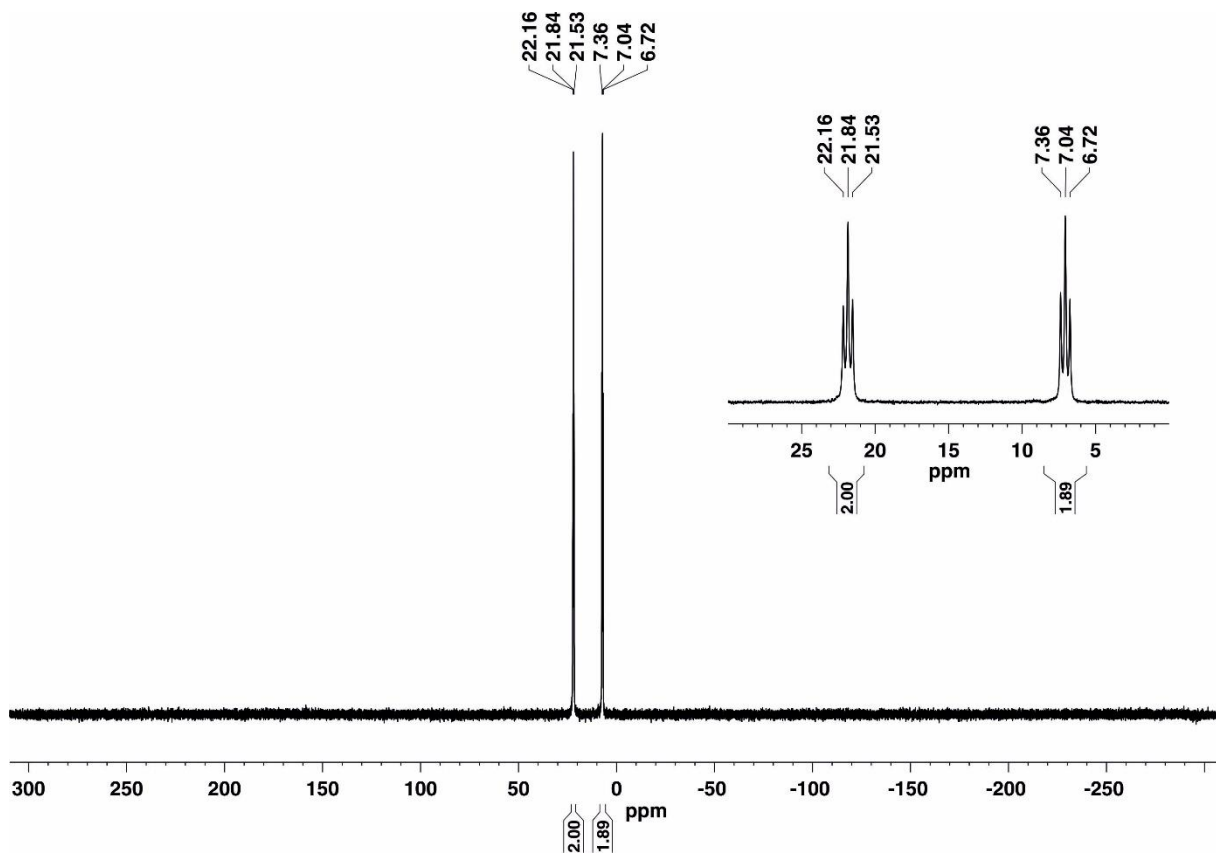


**Figure S12.**  $^{31}\text{P}\{\text{H}\}$  NMR spectrum of complex **4** (161.98 MHz, THF- $\text{d}_8$ , 300 K).

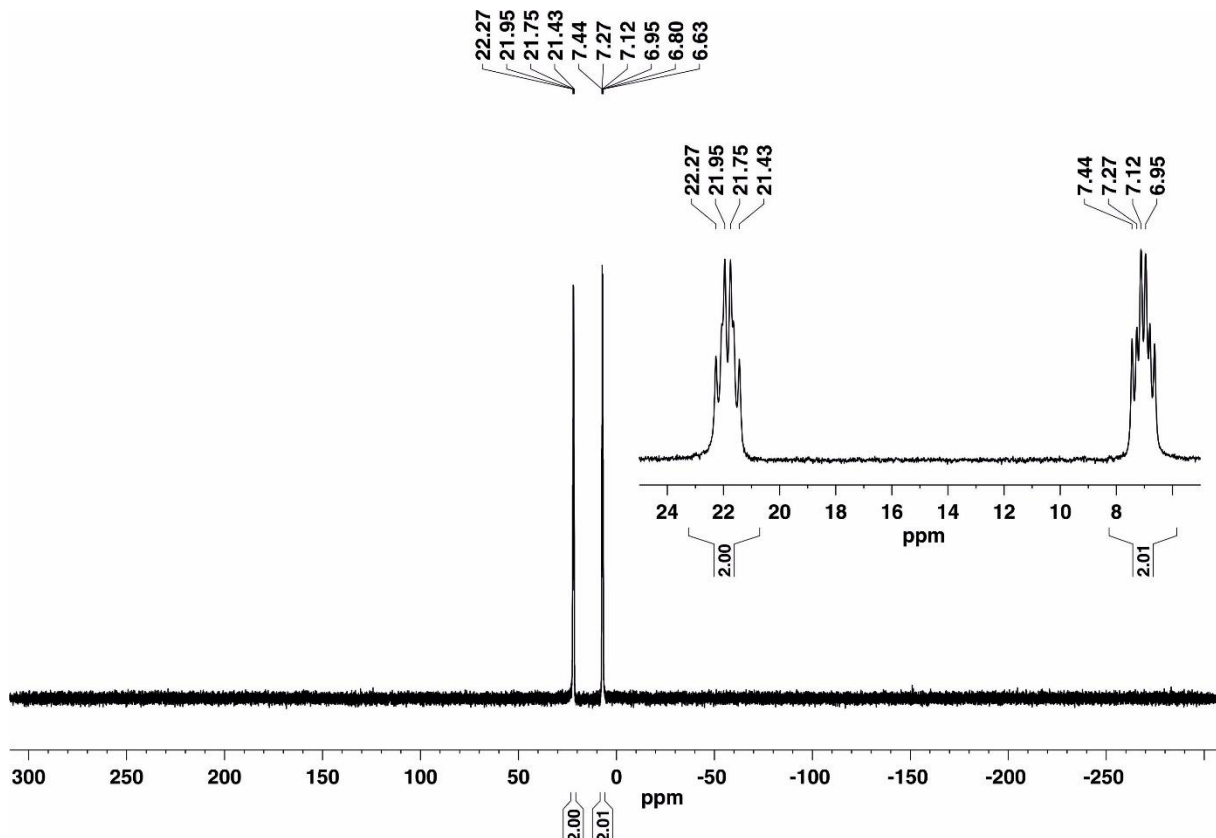


**Figure S13.**  $^{31}\text{P}$  NMR spectrum of complex **4** (161.98 MHz, THF- $\text{d}_8$ , 300 K). Coupling constants with  $J_{\text{P},\text{H}}$  coupling constants of 32 Hz and 27 Hz were extracted by simulation.

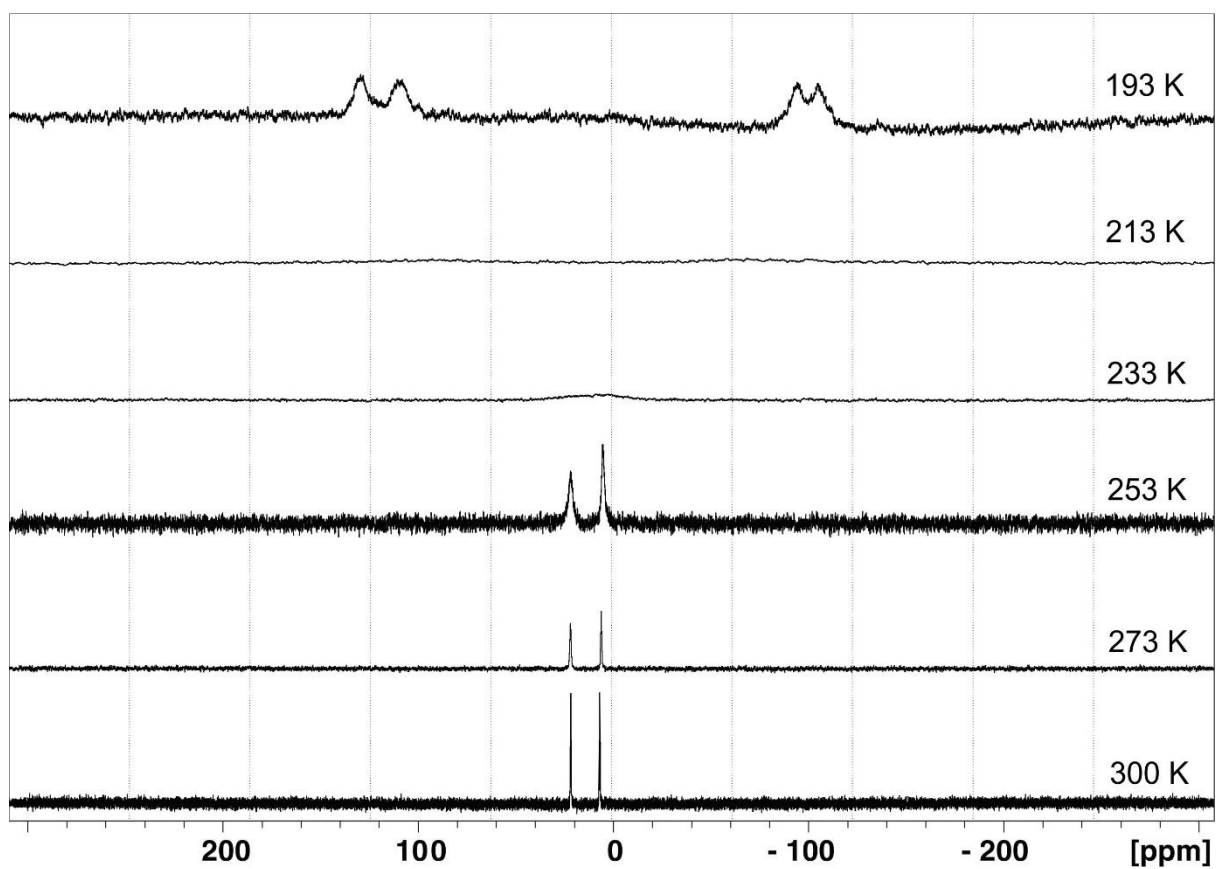


**Figure S14.** Variable temperature  $^{31}\text{P}\{\text{H}\}$  NMR spectrum of **4** (161.98 MHz, THF-d<sub>8</sub>).

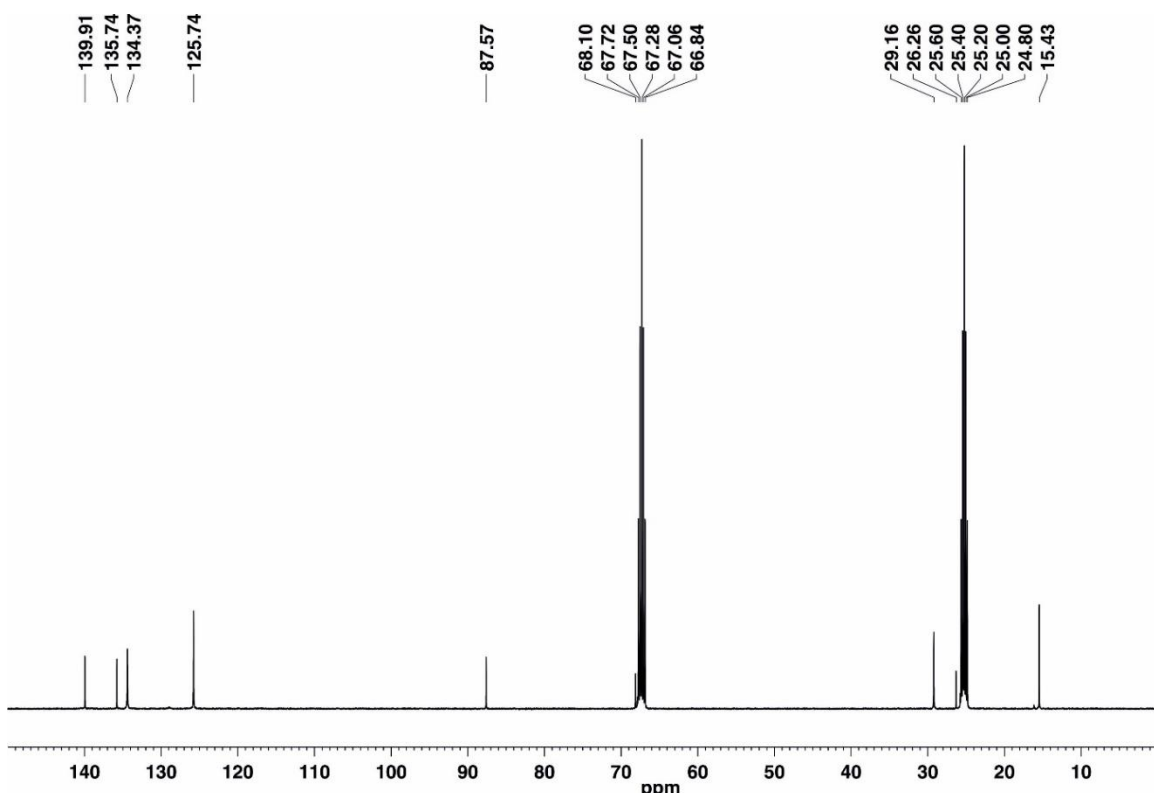


**Figure S15.**  $^{13}\text{C}\{\text{H}\}$  NMR spectrum of complex **4** (100.61 MHz, THF-d<sub>8</sub>, 300 K).

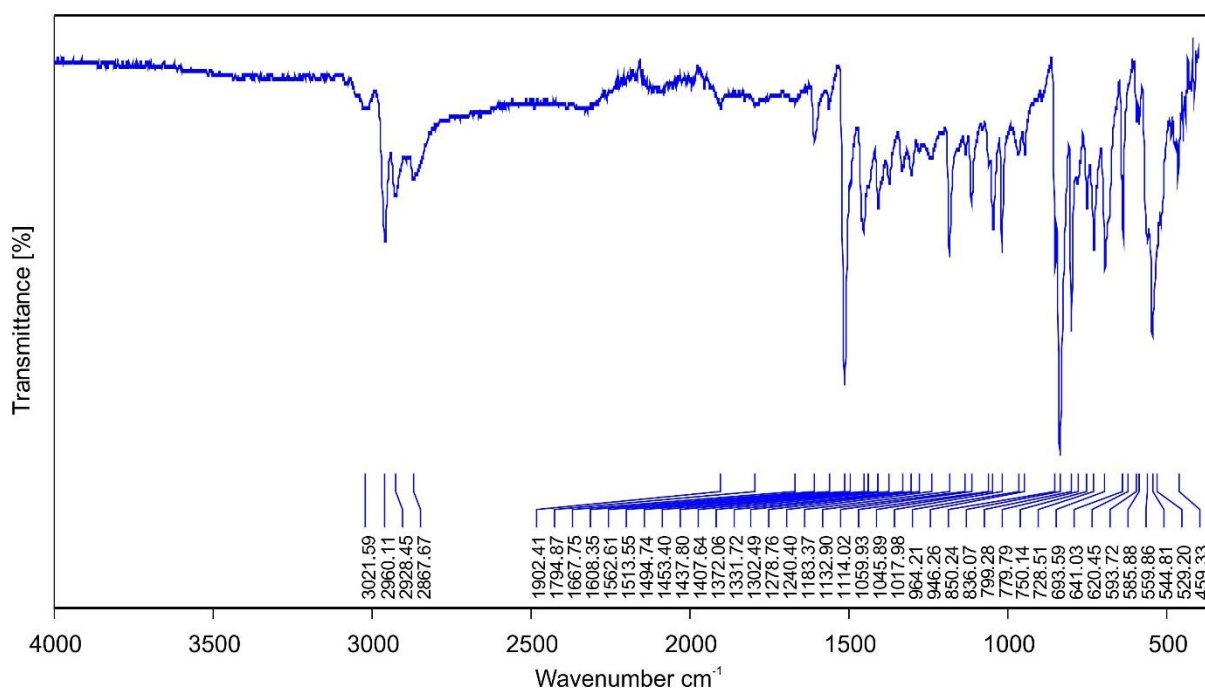


**Figure S16.** Solid-state IR spectrum of complex 4.

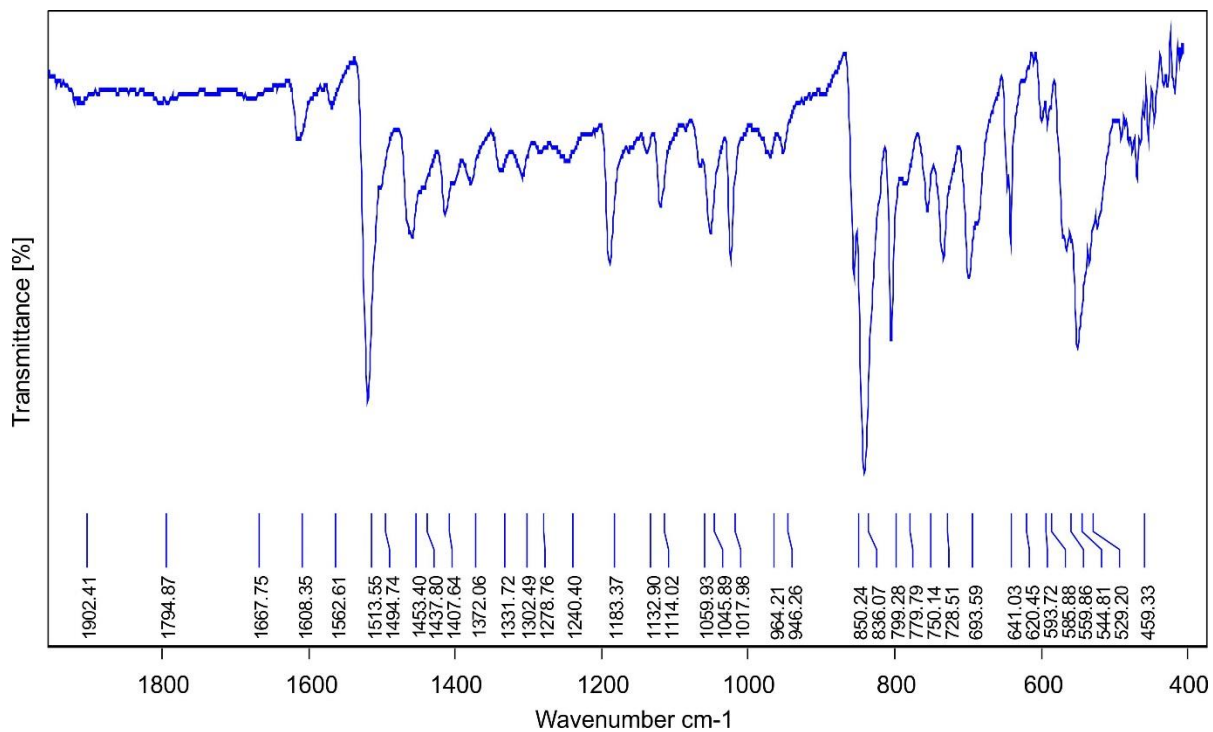


**Figure S17.** Expanded region for the solid-state IR spectrum of complex 4.

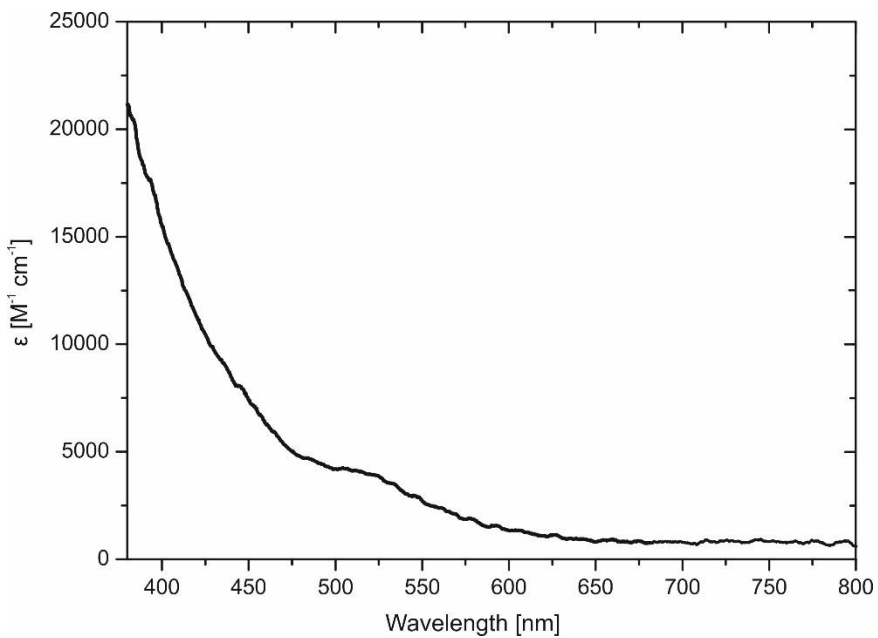


**Figure S18.** UV-vis spectrum of **4** in THF.

### 1.5 Reaction of **3** with Me<sub>3</sub>SiCl

A red solution of **3** (29 mg, 0.016 mmol) in 3 mL of THF was treated with a Me<sub>3</sub>SiCl solution (0.4 mL, 0.152 (M) in THF, 0.061 mmol). The solution turned brown and slowly changed to deep orange over 30 min. The reaction mixture was stirred overnight and evaporated completely. The dark brown residue was dissolved in 0.5 mL of THF-d<sub>8</sub> and analyzed by NMR spectroscopy. The formation of P<sub>7</sub>(TMS)<sub>3</sub>,<sup>2</sup> P(SiMe<sub>3</sub>)<sub>3</sub><sup>3</sup> and PH(SiMe<sub>3</sub>)<sub>2</sub><sup>4</sup> in 1: 0.1: 0.2 was confirmed by <sup>31</sup>P{<sup>1</sup>H} NMR spectroscopy. Another minor product of unknown identity was also observed in the <sup>31</sup>P{<sup>1</sup>H} NMR spectrum, appearing a singlet signal at 115.3 ppm.

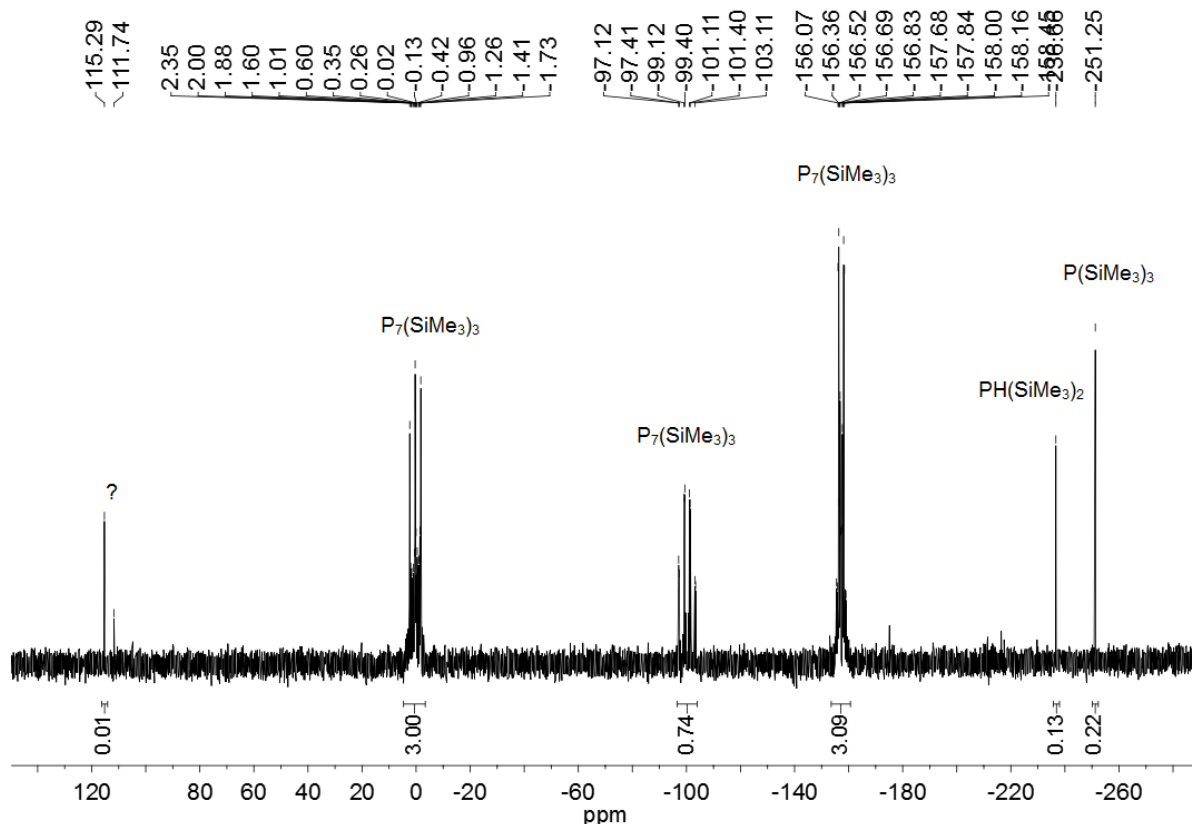


**Figure S19.**  $^{31}\text{P}\{\text{H}\}$  NMR spectrum (161.98 MHz, THF-d<sub>8</sub>, 300 K) of the reaction mixture of **3** with an excess of Me<sub>3</sub>SiCl.

## 2 Crystallographic data for complexes **2**, **3** and **4**

Light green single crystals of **2** suitable for X-ray measurements were obtained by diffusion of diethyl ether into the DME solution. Dark brown single crystals of **3** and **4** were obtained upon diffusion of *n*-hexane into the THF solutions. The crystals were processed at an Xcalibur, AtlasS2, Gemini ultra CCD diffractometer with microfocus Cu radiation (**2**), Agilent Technologies SuperNova Eos CCD device employing microfocus Mo radiation (**3**), or a GV50 TitanS2 CCD device with microfocus Cu radiation (**4**). The CrysAlis software was used to apply gaussian (**2** and **4**) or numerical (**3**) absorption corrections.<sup>5</sup> The PLATON Squeeze model was applied to one highly disordered Et<sub>2</sub>O molecule in the unit cell of **2**. Using Olex2,<sup>6</sup> the structures were solved with direct methods by ShelXT and refined with ShelXL using least squares minimization.<sup>7</sup> Details of the structure determinations are given below. The crystallographic information files (CIF) have been deposited at the CCDC, 12 Union Road, Cambridge, CB21EZ, U.K., and can be obtained on request free of charge, by quoting the publication citation and deposition numbers CCDC 1583278–1583280.

## 2.1 Crystallographic Data of 2

Crystal Data for  $C_{61}H_{79}FeKO_7P_4$  ( $M = 1143.07$  g/mol): monoclinic, space group  $P2_1/c$  (no. 14),  $a = 17.36501(15)$  Å,  $b = 16.04859(13)$  Å,  $c = 22.20094(18)$  Å,  $\beta = 100.9516(8)^\circ$ ,  $V = 6074.36(9)$  Å<sup>3</sup>,  $Z = 4$ ,  $T = 122.8(6)$  K,  $\mu(\text{CuK}\alpha) = 3.989$  mm<sup>-1</sup>,  $D_{\text{calc}} = 1.250$  g/cm<sup>3</sup>, 44698 reflections measured ( $6.84^\circ \leq 2\Theta \leq 133.436^\circ$ ), 10689 unique ( $R_{\text{int}} = 0.0286$ ,  $R_{\text{sigma}} = 0.0236$ ) which were used in all calculations. The final  $R_1$  was 0.0296 ( $I > 2\sigma(I)$ ) and  $wR_2$  was 0.0738 (all data).

## 2.2 Crystallographic Data of 3

Crystal Data for  $C_{110}H_{130}Fe_2Na_2O_5P_4$  ( $M = 1813.69$  g/mol): orthorhombic, space group  $Pnma$  (no. 62),  $a = 23.2636(5)$  Å,  $b = 25.7313(5)$  Å,  $c = 16.0339(4)$  Å,  $V = 9597.9(4)$  Å<sup>3</sup>,  $Z = 4$ ,  $T = 122.99(10)$  K,  $\mu(\text{MoK}\alpha) = 0.432$  mm<sup>-1</sup>,  $D_{\text{calc}} = 1.255$  g/cm<sup>3</sup>, 62104 reflections measured ( $5.988^\circ \leq 2\Theta \leq 56.066^\circ$ ), 10867 unique ( $R_{\text{int}} = 0.0352$ ,  $R_{\text{sigma}} = 0.0289$ ) which were used in all calculations. The final  $R_1$  was 0.0615 ( $I > 2\sigma(I)$ ) and  $wR_2$  was 0.1455 (all data).

The diffraction pattern of a crystal of **3** revealed several strong systematic absence violations. These non-Bragg reflections are of elongated shape in comparison to the round Bragg reflections. We tested lower symmetry and twinning, but could not find a reasonable model.

## 2.3 Crystallographic Data for 4

Crystal Data for  $C_{101.69}H_{110.94}Fe_2NaO_{2.81}P_4$  ( $M = 1636.62$  g/mol): orthorhombic, space group  $Pnma$  (no. 62),  $a = 23.4789(3)$  Å,  $b = 24.3950(2)$  Å,  $c = 16.5309(2)$  Å,  $V = 9468.37(18)$  Å<sup>3</sup>,  $Z = 4$ ,  $T = 123.01(10)$  K,  $\mu(\text{CuK}\alpha) = 3.495$  mm<sup>-1</sup>,  $D_{\text{calc}} = 1.148$  g/cm<sup>3</sup>, 108153 reflections measured ( $6.458^\circ \leq 2\Theta \leq 147.01^\circ$ ), 9716 unique ( $R_{\text{int}} = 0.0450$ ,  $R_{\text{sigma}} = 0.0191$ ) which were used in all calculations. The final  $R_1$  was 0.0836 ( $I > 2\sigma(I)$ ) and  $wR_2$  was 0.2756 (all data).

Several crystals of **4** were processed and revealed high mosaicity together with very weak diffracting power already at low angles. The best solution was found in *Pnma*. Attempts in acentric orthorhombic and different monoclinic space groups resulted similarly disordered models. The structure was refined applying restraints for the disordered parts of the structure. The poor diffraction data did not allow for better refinement. According to the electron density peaks (Figure S20), the position adjacent to the minor sodium site Na2 (22% occupancy) seems to be occupied by THF in the same ratio. In case the Na2 site is unoccupied, *n*-hexane (78%

occupancy) is likely to be located in the void. However, the voids had to be treated with a solvent mask because the disorder could not be refined properly on the crystallographic mirror plane.

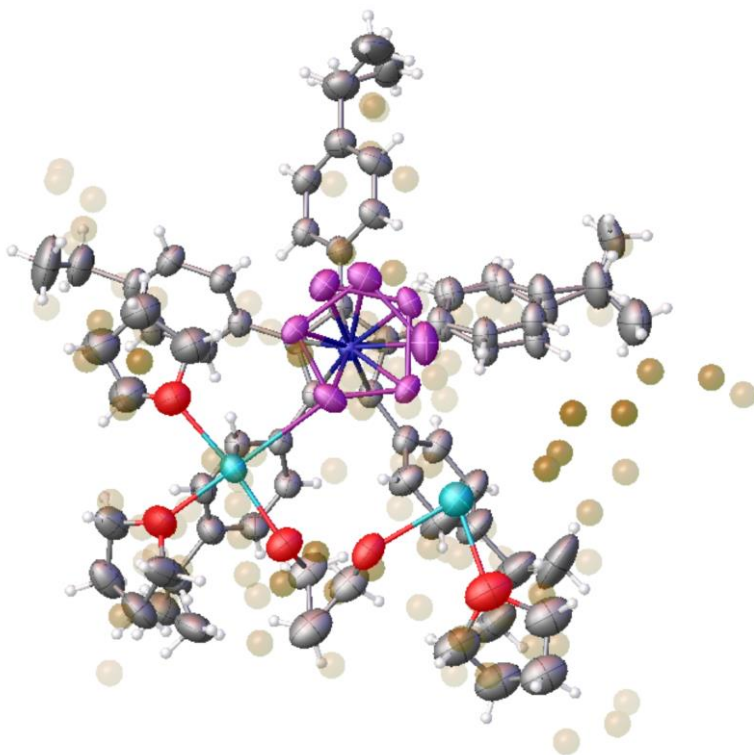


**Figure S20.** Residual density peaks indicating THF/n-hexane disorder.

### 3 DFT calculations

The DFT calculations were performed using Gaussian09, revision D.01<sup>8</sup> at the B3LYP level of theory<sup>9,10</sup> on the truncated model complexes  $[(C_5Ph_5)Fe(\eta^4\text{-}P_4)]$  (**2'**),  $Na[\{(C_5Ph_5)Fe\}_2(\mu,\eta^{4:4}\text{-}P_4)(H)]$  (**4'**) and  $Na[\{CpFe\}_2(\mu,\eta^{4:4}\text{-}P_4)(H)]$  (**4A**). The structure of **2'** was optimized using the LANL4DZ basis set for Fe and the 6-31G(d,p) basis set for the C, H, and P atoms.<sup>11,12</sup> Molecular orbitals were visualized via the program Gabedit.<sup>13</sup> The isosurface value is set to 0.05. **4'** and **4A** were optimized using the 6-311G(d,p) basis set for all atoms.<sup>12</sup> The nature of each stationary point was validated by frequency calculations.

The Synchronous Transit-Guided Quasi-Newton (STQN) Method was used for the transition state search.<sup>14</sup> The QST2 optimizations were performed at the B3LYP level of theory using 6-311G(d,p) basis set for all atoms. One imaginary frequency was found for the transition state structure **4TS** ( $-603\text{ cm}^{-1}$ ), which corresponds to the nuclear motion along the reaction coordinate. Intrinsic reaction coordinate (IRC) calculations were conducted to confirm the transition states.

### 3.2 Calculated frontier molecular orbitals of **2'**

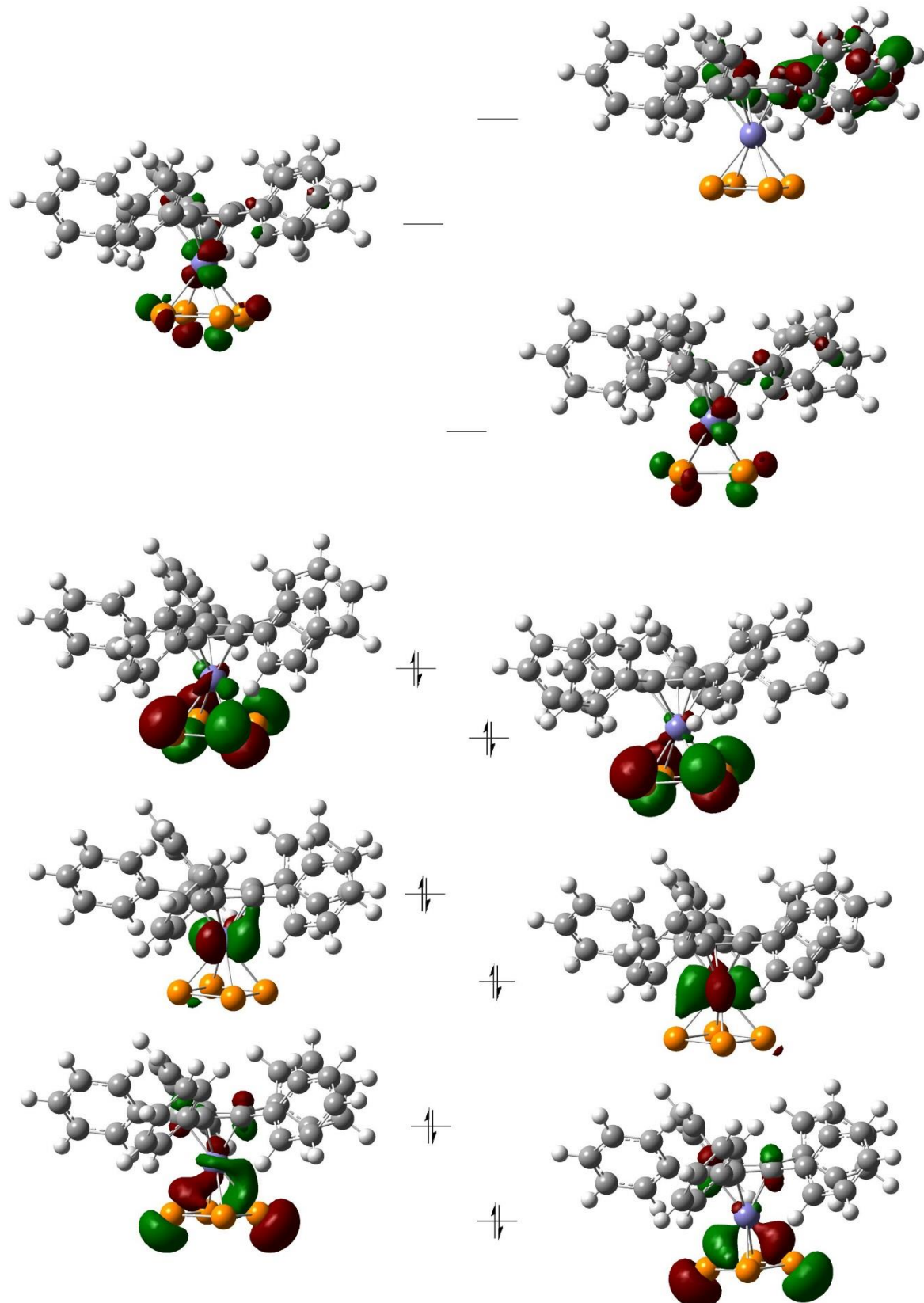


**Figure S21.** Molecular Kohn-Sham orbitals of **2'**.

### 3.3 Optimization of isomers of Na[CpFe<sub>2</sub>P<sub>4</sub>H] (4A)

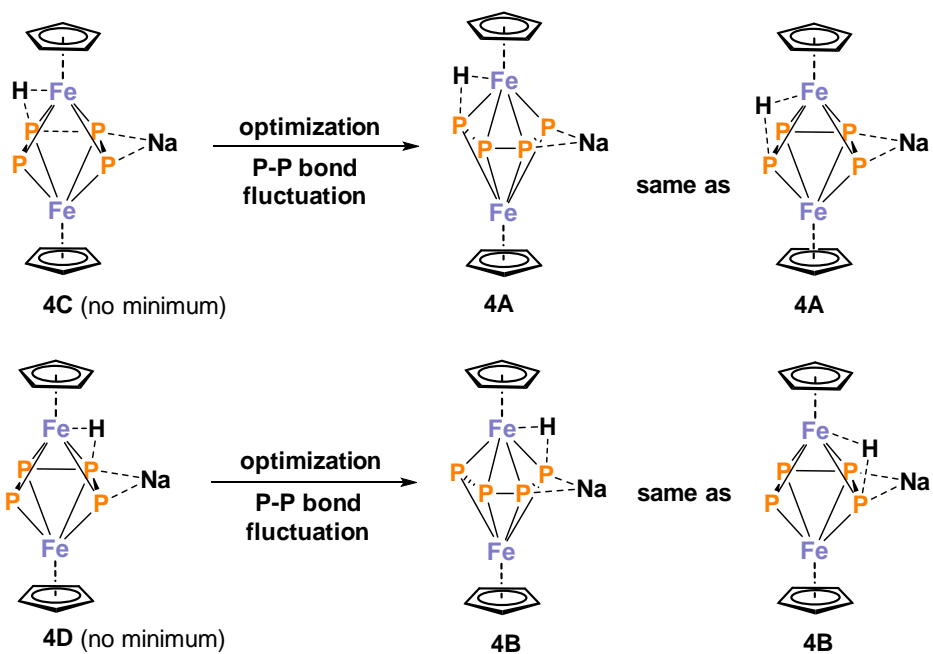


**Figure S22.** Optimization of isomers of isomeric complexes **4C** and **4D** yielded **4A** and **4B**, respectively.

### 3.4 Calculated energy profile for the fluxional behaviour of **4A**

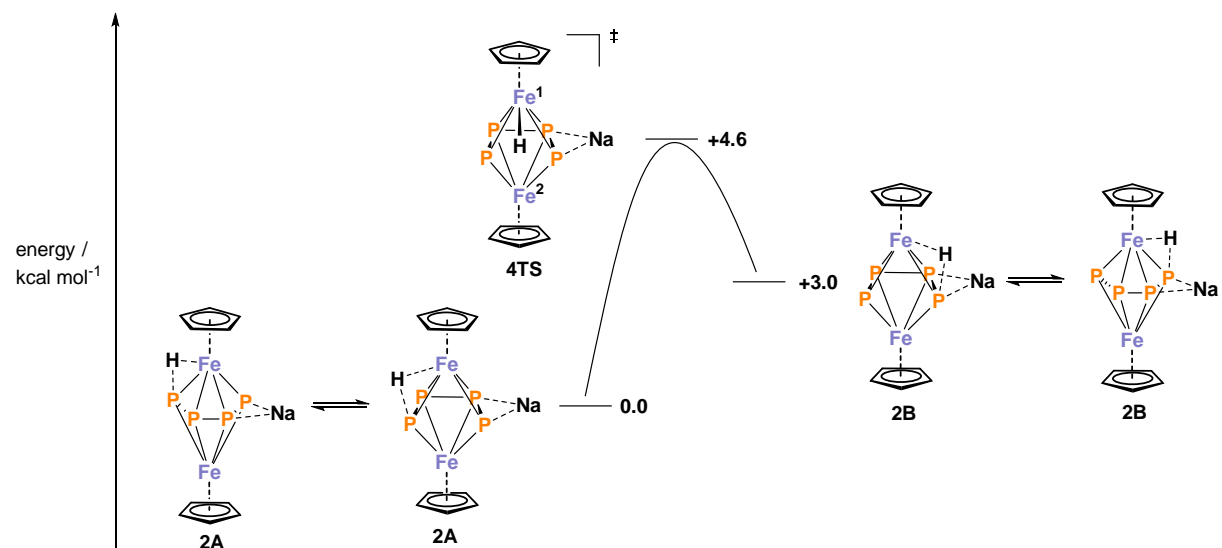


**Figure S23.** Calculated energy profile for the fluctional behaviour of **4A**.

### 3.6 TD-DFT calculations for complex 2'

**Table S1.** Calculated electronic transitions of **2'** at the B3LYP/def2-TZVP level of theory. The relevant molecular orbitals are depicted in Figures S20.

No.	$\nu$ [nm]	$f$	%	Transition	Exp. $\nu$ [nm]
<b>1</b>	658.4	0.002055	26	HOMO → LUMO	650
			29	HOMO → LUMO+2	
<b>2</b>	654.2	0.001603	28	HOMO → LUMO	650
			25	HOMO → LUMO+2	
			11	HOMO → LUMO+13	
<b>3</b>	442.0	0.000790	26	HOMO-4 → LUMO	405
			28	HOMO-3 → LUMO	
			17	HOMO → LUMO+1	
<b>4</b>	362.6	0.012134	93	HOMO → LUMO+2	405
<b>5</b>	353.6	0.012732	15	HOMO-3 → LUMO+5	405
			57	HOMO → LUMO+3	

## 4 Cartesian coordinates of the optimized structures

### 4.1 Cartesian coordinates of 2'

Final Single Point Energy = -2837.242569 Hartree

Fe	0.00000000	0.00000000	0.00000000
P	0.00000000	0.00000000	2.39877984
P	1.95054319	0.00000000	1.39424466
P	-0.51450789	1.88127445	1.40080075
P	1.43271589	1.88374236	0.39609323
C	-1.80695139	-0.60936747	-0.83223690
C	-1.05448946	0.16603836	-1.79268797
C	-1.02201141	-1.77146447	-0.48636883
C	0.19286439	-0.51957265	-2.03608791
C	0.21195757	-1.71427711	-1.23004311
C	-3.20127436	-0.34755947	-0.39336589
C	-1.55543065	1.34908994	-2.54047879
C	-1.45721683	-2.91215412	0.35859766
C	1.17754126	-0.17021009	-3.09404605
C	1.23686859	-2.78635872	-1.31436922
C	-4.21071529	-0.14747640	-1.35106404
C	-3.56623820	-0.34689209	0.96347568
C	-1.58405025	1.32214849	-3.94647499
C	-2.06530589	2.48539269	-1.89073146
C	-2.69482540	-3.53397359	0.12020827
C	-0.63059903	-3.44712707	1.36141448
C	1.76508870	1.10203350	-3.18732088
C	1.48629826	-1.11619780	-4.08842846
C	0.84367281	-4.10590031	-1.59936900
C	2.61057635	-2.51888690	-1.19454516
H	-3.94871455	-0.14638284	-2.40491820
C	-5.53801041	0.05260160	-0.96743756
H	-2.79639643	-0.49289866	1.71425933
C	-4.89302516	-0.15315519	1.34591417
C	-2.09615640	2.39502414	-4.67733559
H	-1.19933469	0.45107430	-4.46850933
C	-2.58062783	3.55563858	-2.62189424
H	-2.04020600	2.52330048	-0.80649057
H	-3.34642247	-3.13941354	-0.65357844
C	-3.09693582	-4.64562206	0.86312689
H	0.32177081	-2.97081113	1.56536604
C	-1.02836034	-4.56180459	2.09743219
H	1.54987419	1.83519481	-2.41745800
C	2.63273494	1.41287822	-4.23461791
C	2.35687023	-0.80567964	-5.13366680

H	1.03867277	-2.10417192	-4.03708157
H	-0.21289554	-4.33369586	-1.70277111
C	1.78747430	-5.12289129	-1.75115407
C	3.55400403	-3.53372875	-1.35160064
H	-6.29925950	0.21032500	-1.72841603
C	-5.88619087	0.04928462	0.38410970
H	-5.14928096	-0.15301370	2.40279196
H	-2.10201192	2.35033628	-5.76426235
C	-2.59812899	3.51836301	-4.01789465
H	-2.96478368	4.42578197	-2.09437119
H	-4.06261279	-5.10454573	0.66251551
C	-2.26456788	-5.16622373	1.85475301
H	-0.37215603	-4.95348930	2.87108930
H	3.07861876	2.40383556	-4.28064340
C	2.93498202	0.46264700	-5.21249049
H	2.58185430	-1.55778452	-5.88678237
H	1.45463107	-6.13582791	-1.96695749
C	3.14920253	-4.84173768	-1.62860850
H	4.61109236	-3.30003828	-1.24850150
H	2.92932383	-1.51064657	-0.95773959
H	3.88663049	-5.63296957	-1.74471820
H	-2.57629646	-6.03188365	2.43503198
H	3.61514539	0.70680667	-6.02559831
H	-6.91948975	0.20660170	0.68567201
H	-2.99578422	4.35669165	-4.58578159

## 4.2 Cartesian coordinates of 4' (optimized at the B3LYP/def2-TZVP level of theory)

Fe	0.75311134249197	-0.83548897688584	0.43226994206723
P	0.61090387945682	1.00604909957737	2.12656790686497
P	1.44089065035865	0.78091702642775	-1.27173432803565
P	2.35548220221366	0.76335981303190	0.94350817006958
P	-0.52938330649761	0.82469014944266	-0.72280373927897
C	1.83217040813696	-2.51398274103246	1.11933524265331
C	0.48448692245448	-2.57263842523987	1.59328577742054
C	0.40492707159341	-2.57121409409097	-0.71729333848052
C	1.78302894446555	-2.50006203067839	-0.31980368756842
C	-0.39847299469723	-2.59746673103788	0.46307587149136
Fe	0.87471648686252	2.43042731736595	0.32011143793096
C	3.03530320273836	-2.46228152101640	1.96671624448285
C	0.05475527372755	-2.75236269452954	2.99516433813180
C	-0.07907373109241	-2.77241168134110	-2.09550229382155
C	2.92695982431615	-2.59669983104226	-1.25182773278382
C	-1.86245019686089	-2.78726378812976	0.51885774024925
C	1.41641989316473	4.13057903346958	1.38971202045432
C	-0.01011358926972	4.13313677853518	1.13546623837220
C	1.07016027127404	4.17493788120255	-0.90894565855093
C	2.07184963805506	4.14167469282279	0.10590963131605
C	-0.21315816820083	4.16940307339040	-0.27923274754881
C	3.01681079472193	-1.80320161189859	3.20650931784928
C	4.22894234425413	-3.07538916016791	1.57487050966157

C	-0.93072895016331	-1.96206405843058	3.58873516960191
C	0.60293726935216	-3.80452086805849	3.73426920194236
C	0.42849694860313	-2.05316001037408	-3.17997036195164
C	-1.01344682812318	-3.78249087477420	-2.34428617278155
C	3.96765781942074	-1.66711489419533	-1.27403330924969
C	2.98862621671752	-3.68612622997309	-2.12604824851492
C	-2.39803156377693	-3.82997565189851	1.27979757894332
C	-2.73188893027541	-1.99043967537623	-0.22899511014436
C	2.07842078784801	4.05821790830612	2.70508579561627
C	-1.10254748932597	4.24095450496542	2.12490191282368
C	1.34750506572011	4.41388378358676	-2.33819847246125
C	3.50640095023584	4.36039420595053	-0.20274447787772
C	-1.50445636567235	4.27363172395553	-0.98455353784574
Na	3.32680059218884	1.21469734717274	3.44557533453056
H	2.09621060394709	-1.35172662567842	3.54819717009150
C	4.15512626701443	-1.73862437152612	4.00094530935471
H	4.26911216599981	-3.61611898248803	0.64234898407329
C	5.37204537143272	-2.99487976142302	2.36146354922786
H	-1.37937497867579	-1.15647223183000	3.02716216910323
C	-1.34598140218482	-2.20852801398468	4.89129110644394
H	1.35920450274293	-4.43032634361856	3.27973006902400
C	0.18690081331682	-4.05387076048349	5.03472587131877
H	1.14785209774408	-1.26642711769283	-3.00865693150004
C	0.02220374273330	-2.34425434449668	-4.47512814414683
H	-1.41559142055204	-4.35222083383422	-1.51937768686686
C	-1.42395402465673	-4.06930812589234	-3.63800328060806
H	3.93474870861164	-0.82157935874034	-0.60364655474599
C	5.03769081182955	-1.82142887941509	-2.14457319307864
H	2.18442892577383	-4.40912216002200	-2.13097485032467
C	4.05970165418226	-3.84378640505822	-2.99506045612097
C	-3.76581244231617	-4.07460611139840	1.28867101651863
C	-4.09740017685258	-2.23620033004826	-0.22253099221229
C	1.40034776137332	3.59929200142609	3.85246465282138
C	3.43642930054991	4.39210210445206	2.86726247095722
C	-2.13206283815514	3.29965403039208	2.17877033181489
C	-1.15513793625065	5.34427086915893	2.98072684857524
C	2.25934193866672	3.64446339266947	-3.06178910545368
C	0.73313663264383	5.49492508213000	-2.97913739829291
C	4.45106957887466	3.33942687972087	-0.27621132946662
C	3.92228168308789	5.67151383500726	-0.45355354426339
C	-2.52078558694867	5.10533614254328	-0.50469675404342
C	-1.72729835470713	3.57625898218909	-2.17744307901603
H	0.36076686456265	3.33027228608167	3.78681372262853
H	4.10442615616067	-1.26479228302622	4.97710537964436
C	5.34747122114310	-2.32244081245476	3.57632574732209
H	6.28208930495566	-3.47202438578327	2.02056376142800
H	-2.10917113224243	-1.58193012057329	5.33464381883227
C	-0.78973466572284	-3.25487895964673	5.61925053852137
H	0.62225670321766	-4.87531909968329	5.58934791700961
H	0.43200525801160	-1.77698134662351	-5.30126939300734
C	-0.90423549227671	-3.35470080137773	-4.71130312920865
H	5.83062111792148	-1.08410520620291	-2.15247011496784
C	5.09036569991318	-2.91120425367542	-3.00702452214991
H	4.08605677805463	-4.69290102098656	-3.66593349082209
C	-4.62067778087447	-3.28184905813623	0.53148846321472
H	-0.95488490736517	2.93259597328628	-2.56953405451364
C	-2.92939054710359	3.69550688984786	-2.85798450945166
H	-3.08146116399654	3.13749612268997	-3.77325613465053

C	2.04661848795862	3.45741420616759	5.07619009872460
H	3.99642961125692	4.77873789740911	2.03305662481673
C	4.08724015601620	4.23466421523641	4.08807429527111
H	-2.09263409659253	2.44835820785722	1.51310272145867
C	-3.18646810119530	3.45899488451222	3.06727469326206
H	-0.36087252129661	6.07935285904399	2.94624855941801
C	-2.20913333165912	5.50371656489455	3.87129341072311
H	2.73590258610823	2.80046351426037	-2.58724829148089
C	2.55466831750459	3.94928790806777	-4.38401452400767
H	0.02199473275493	6.09922870655845	-2.43270342500420
C	1.02928360299555	5.80191086632568	-4.29952812037242
H	4.13802860440732	2.32013128589460	-0.10958963284693
C	5.78166397729638	3.62358210365100	-0.55989796597672
H	3.19051162366657	6.46879040753043	-0.42608113754717
C	5.25016208652018	5.95821217396868	-0.73776745866981
H	-2.36966234317453	5.66744315243718	0.40477661347420
C	-3.72624696167510	5.22211204861668	-1.18484454922204
C	-3.93753487024240	4.51657678567344	-2.36370009835270
H	1.48326995863425	3.10376526304323	5.93095089086127
C	3.40156112449255	3.76223698293263	5.20619738290824
H	-3.97849566447963	2.72146580101802	3.09626634913968
C	-3.23146815046854	4.56223301940522	3.91410754600117
H	-2.23590559420401	6.36555868341678	4.52608131520879
H	3.26192110190844	3.33526418863695	-4.92705396632149
C	1.94137190015536	5.02834939707545	-5.01000114442696
H	0.54413331570402	6.64493446514243	-4.77506209555320
H	6.50056624713521	2.81541440163093	-0.61565946273161
C	6.18934095780137	4.93299890234656	-0.78321280074045
H	5.55154211896670	6.98013593908831	-0.93045829869692
H	-4.50025884159739	5.86843839162339	-0.79019074804145
H	2.18104430028054	5.27265008749061	-6.03740646418576
H	3.90239669523828	3.66282260326696	6.16086186193626
H	5.13201889927027	4.50857234778327	4.16822796410606
H	7.22578599634899	5.15209522794081	-1.00678801885452
H	-4.87633641535605	4.61074429276259	-2.89471380742392
H	-4.05683319928535	4.68814997163015	4.60315273932087
H	5.92504970130226	-3.03128902216147	-3.68579972183014
H	6.23353161965029	-2.27449438267351	4.19605664619790
H	-1.12249570767623	-3.45464092271588	6.63004324298736
H	-1.73781306373437	-4.45636128985056	1.86364193022217
H	-5.68532741834134	-3.47991886075837	0.52827054755949
H	-4.16185349170964	-4.88749963116918	1.88393770577879
H	-4.75380479105114	-1.60912504240617	-0.81287406113052
H	-2.33044118037594	-1.17788924604807	-0.81651046580415
H	-2.14732320437784	-4.85687073976046	-3.80638953999953
H	-1.22112488635255	-3.58555796014332	-5.72093473491215
H	-0.26026138852888	-0.11174993147870	1.51662498016538

### 4.3 Cartesian Coordinates of 4A

Final Single Point Energy = -4442.857279 Hartree

Fe	-1.60084434	-0.19645746	-0.05162000
P	0.00037471	1.22562754	-1.05460519
P	0.03192836	-1.39313273	1.21817729

P	0.00382044	1.05288340	1.07185168
P	-0.20524664	-1.87978000	-0.81993975
C	-3.28670864	0.87714059	-0.62710411
C	-3.28314543	-0.41932500	-1.21900878
C	-3.29697017	-0.67029518	1.07745937
C	-3.29773252	0.72232212	0.78676777
C	-3.29187378	-1.37600181	-0.15803736
Fe	1.62274417	-0.22599901	-0.12399742
C	3.31372569	0.94052060	-0.37668400
C	3.37361856	-0.20889461	-1.21049730
C	3.26502556	-0.92082393	0.98327329
C	3.23500899	0.50284523	0.97756175
C	3.34037651	-1.36168006	-0.36150537
Na	0.04789839	3.67221275	0.05733917
H	-3.26278666	1.81250162	-1.16571261
H	-3.28370282	1.51679935	1.51785541
H	-3.27702581	-1.11246228	2.06175757
H	-3.27769110	-2.44933976	-0.27282479
H	-3.27133770	-0.63706964	-2.27569638
H	3.43030098	-0.21216920	-2.28812822
H	3.33050736	-2.38994447	-0.69011616
H	3.19259318	-1.55277288	1.85447903
H	3.15524909	1.13492838	1.84828700
H	3.30089664	1.96472671	-0.71734724
H	0.97561724	-1.08449078	-1.40284369

#### 4.4 Cartesian Coordinates of 4B

Final Single Point Energy = -4442.852584 Hartree

Fe	-1.62214430	-0.14433681	-0.04731619
P	-0.17380519	1.30048074	-1.11721049
P	-0.05271180	-1.41923460	1.20747692
P	0.02898727	1.09566078	1.03838483
P	-0.07740684	-1.77427056	-0.81387687
C	-3.34293725	0.92217371	-0.49123085
C	-3.29524734	-0.29704062	-1.23684915
C	-3.30355194	-0.81985455	1.01177449
C	-3.35124218	0.59600868	0.89234343
C	-3.27225221	-1.37055556	-0.30189058
Fe	1.59665958	-0.21532504	-0.12142323
C	3.40219680	0.71894065	-0.54310541
C	3.32690003	-0.55402109	-1.19903558
C	3.15999825	-0.89800530	1.07236489
C	3.31248673	0.50044539	0.85479176
C	3.18278251	-1.54774388	-0.19699744

Na	0.46062341	3.65108179	0.19821575
H	-3.36567492	1.91729679	-0.91043384
H	-3.35939780	1.29734669	1.71311252
H	-3.27137907	-1.37765308	1.93498226
H	-3.20355471	-2.41953721	-0.54523348
H	-3.27569137	-0.38814103	-2.31190040
H	3.36691683	-0.72517453	-2.26383897
H	3.05870861	-2.60585933	-0.36677872
H	3.03565588	-1.38134800	2.02836017
H	3.31532798	1.25780221	1.62392770
H	3.50730667	1.67414268	-1.03691506
H	0.99677501	0.39880330	-1.55303986

#### 4.5 Cartesian Coordinates of 4TS

**Final Single Point Energy = -4442.850825 Hartree**

Fe	-1.62345603	-0.14749528	-0.04430752
P	-0.05302153	1.25046247	-1.07388510
P	-0.05477072	-1.43688107	1.20007727
P	0.00414288	1.09192866	1.05708414
P	-0.13383347	-1.80251433	-0.82267133
C	-3.31094778	0.95030750	-0.54580700
C	-3.29054690	-0.29574401	-1.24302803
C	-3.33021968	-0.73206346	1.02476038
C	-3.33823813	0.67937465	0.84954362
C	-3.30392059	-1.33379874	-0.26556186
Fe	1.58838243	-0.23416605	-0.13438987
C	3.37215991	0.78361405	-0.46246640
C	3.36115569	-0.44860842	-1.18105402
C	3.15542818	-0.93196884	1.05930292
C	3.24825891	0.48139629	0.92219157
C	3.22715850	-1.50758586	-0.24088531
Na	0.45366752	3.64754098	0.12269574
H	-3.29324272	1.92823836	-1.00322249
H	-3.33522680	1.41221536	1.64234576
H	-3.32103465	-1.25409750	1.96925589
H	-3.26848620	-2.39341128	-0.46741281
H	-3.26589614	-0.42789150	-2.31368103
H	3.42607736	-0.55766375	-2.25291443
H	3.15310198	-2.55822452	-0.47433674
H	3.02640209	-1.47104024	1.98440545
H	3.20606132	1.19355125	1.73196670
H	3.46060852	1.76635107	-0.90124975
H	0.95372058	-0.25225827	-1.52972746

- 
- (1) U. Chakraborty, M. Modl, B. Mühlendorf, M. Bodensteiner, S. Demeshko, N. J. C. van Velzen, M. Scheer, S. Harder and R. Wolf, *Inorg. Chem.*, 2016, **55**, 3065.
- (2) H. Schmidbaur and A. Bauer, *Phosphorus, Sulfur, and Silicon and the Related Elements*, 1995, **102**, 217.
- (3) (a) A. A. Prishchenko, M. V. Livantsov, O. P. Novikova, L. I. Livantsova and V. S. Petrosyan, *Heteroatom Chem.*, 2010, **21**, 441; (b) E. Niecke and H. Westermann, *Synthesis*, 1988, 330. (c) G. Fritz and J. Härrer, *Z. Anorg. Allg. Chem.*, 1983, **500**, 14.
- 4 (a) D. C. Gary and B. M. Cossairt, *Chem. Mater.*, 2013, **25**, 2463; (b) H. Bürger and U. Goetze, *J. Organomet. Chem.*, 1968, **12**, 451.
- (5) CrysAlisPro Software System, Agilent Technologies UK Ltd, Yarnton, Oxford, UK, **2013**.
- (6) O. V. Dolomanov, L. J. Bourhis, R. J. Gildea, J. A. K. Howard, H. Puschmann, *J. Appl. Cryst.*, 2009, **42**, 339.
- (7) G. M. Sheldrick, *Acta Cryst.*, 2008, **A64**, 112.
- (8) *Gaussian 09, Revision D.01*, M. J. Frisch, G. W. Trucks, H. B. Schlegel, G. E. Scuseria, M. A. Robb, J. R. Cheeseman, G. Scalmani, V. Barone, B. Mennucci, G. A. Petersson, H. Nakatsuji, M. Caricato, X. Li, H. P. Hratchian, A. F. Izmaylov, J. Bloino, G. Zheng, J. L. Sonnenberg, M. Hada, M. Ehara, K. Toyota, R. Fukuda, J. Hasegawa, M. Ishida, T. Nakajima, Y. Honda, O. Kitao, H. Nakai, T. Vreven, J. A. Montgomery, Jr., J. E. Peralta, F. Ogliaro, M. Bearpark, J. J. Heyd, E. Brothers, K. N. Kudin, V. N. Staroverov, T. Keith, R. Kobayashi, J. Normand, K. Raghavachari, A. Rendell, J. C. Burant, S. S. Iyengar, J. Tomasi, M. Cossi, N. Rega, J. M. Millam, M. Klene, J. E. Knox, J. B. Cross, V. Bakken, C. Adamo, J. Jaramillo, R. Gomperts, R. E. Stratmann, O. Yazyev, A. J. Austin, R. Cammi, C. Pomelli, J. W. Ochterski, R. L. Martin, K. Morokuma, V. G. Zakrzewski, G. A. Voth, P. Salvador, J. J. Dannenberg, S. Dapprich, A. D. Daniels, O. Farkas, J. B. Foresman, J. V. Ortiz, J. Cioslowski, D. J. Fox, *Gaussian, Inc.*, Wallingford CT, **2013**.
- (9) F. Weigend, R. Ahlrichs, *Phys. Chem. Chem. Phys.* 2005, **7**, 3297.
- (10) A. Schäfer, H. Horn, R. Ahlrichs, *J. Chem. Phys.* 1992, **97**, 2571.
- (11) a) P. J. Hay, W. R. Wadt, *J. Chem. Phys.* 1985, **82**, 270; b) P. J. Hay, W. R. Wadt, *J. Chem. Phys.* 1985, **82**, 299.
- (12) a) R. Ditchfield, W. J. Hehre, J. A. Pople, *J. Chem. Phys.* 1971, **54**, 724–728; b) W. J. Hehre, R. Ditchfield, J. A. Pople, *J. Chem. Phys.* 1972, **56**, 2257–2261; c) P. C. Hariharan, J. A. Pople, *Theor. Chem. Acc.* 1973, **28**, 213–222; d) P. C. Hariharan, J. A. Pople, *Mol. Phys.* 1974, **27**, 209–214; e) M. S. Gordon, *Chem. Phys. Lett.* 1980, **76**, 163–168; f) M. M. Franci, W. J. Pietro, W. J. Hehre, J. S. Binkley, D. J. DeFrees, J. A. Pople, M. S. Gordon, *J. Chem. Phys.* 1982, **77**, 3654–3665; g) R. C. Binning Jr., L. A. Curtiss, *J. Comp. Chem.* 1990, **11**, 1206–1216; h) J.-P. Blaudeau, M. P. McGrath, L. A. Curtiss, L. Radom, *J. Chem. Phys.* 1997, **107**, 5016–5021; i) V.

- 
- A. Rassolov, J. A. Pople, M. A. Ratner, T. L. Windus, *J. Chem. Phys.* 1998, **109**, 1223–1229; j)  
V. A. Rassolov, M. A. Ratner, J. A. Pople, P. C. Redfern, L. A. Curtiss, *J. Comp. Chem.* 2001,  
**22**, 976–984; k) T. Clark, J. Chandrasekhar, G. W. Spitznagel, P. v. R. Schleyer, *J. Comp. Chem.*  
1983, **4**, 294–301.  
(13) A.-R. Allouche, *J. Comput. Chem.* 2011, **32**, 174.  
(14) a) C. Peng and H. B. Schlegel, *Israel J. of Chem.* 1993, **33**, 449; b) C. Peng, P. Y. Ayala, H. B.  
Schlegel, M. J. Frisch, *J. Comp. Chem.* 1996, **17**, 49.